TARGETED DELIVERY OF ATORVASTATIN BY APTAMER GATED SILICA NANOPARTICLES IN ATHEROSCLEROSIS CELL CULTURE MODEL

by
Elif Öztemiz

Submitted to Graduate School of Natural and Applied Sciences
in Partial Fulfillment of the Requirements
for the Degree of Master of Science in
Biotechnology

Yeditepe University
2022

TARGETED DELIVERY OF ATORVASTATIN BY APTAMER GATED SILICA NANOPARTICLES IN ATHEROSCLEROSIS CELL CULTURE MODEL

APPROVED BY:

Assoc. Prof. Dr. Bilge Güvenç Tuna ……
(Thesis Supervisor)
(Yeditepe University)

Prof. Dr. Soner Doğan ……
(Thesis Co-Supervisor)
(Yeditepe University)

Prof. Dr. Aydan Dağ ……
(Bezmialem Vakıf University)

Assist. Prof. Dr. Gülnihal Özcan ……
(Koç University)

Prof. Dr. Veli Cengiz Özalp ……
(Atılım University)

DATE OF APPROVAL: ..../..../20...

I hereby declare that this thesis is my own work and that all information in this thesis has been obtained and presented in accordance with academic rules and ethical conduct. I have fully cited and referenced all material and results as required by these rules and conduct, and this thesis study does not contain any plagiarism. If any material used in the thesis requires copyright, the necessary permissions have been obtained. No material from this thesis has been used for the award of another degree.

I accept all kinds of legal liability that may arise in case contrary to these situations.

Elif OZTEMIZ

Signature…..……..……

ACKNOWLEDGEMENTS

First of all, I would like to express my gratitude to my supervisors Asst. Prof. Dr. Bilge GÜVENÇ TUNA and Assoc. Prof. Dr. Soner DOĞAN for their continuous support and motivation during my studies. Especially under the pressure of the global pandemic, they provided me with numerous opportunities to improve my scientific skills. They will always be inspiring role models for my future career. Additionally, I would like to thank Assoc. Prof. Dr. Veli Cengiz ÖZALP for providing nanoparticles used in the present study and his support during my research.

I would like to thank my fellow friends and classmates since undergraduate, Elif YILMAZ and Atakan AYDEN, who have made everything much easier and more joyous during this period. In addition, I wish to show my appreciation for Dilara DURDABAK for her help with the nanoparticle characterization experiments and all the lab members for their endless help and support during my studies.

Last but not the least, my family deserves endless gratitude for their continuous support. Especially, my mom who patiently listened and tried to understand the scientific things I talk about all the time, without her motivational speeches none of this indeed would be possible.

I was awarded the 2210-C Primary Research Area scholarship by the Scientific and Technological Research Council of Turkey (TUBITAK) for a year starting from March 2021.

This project was funded by L'Oréal-UNESCO for Women in Science Young Talents Programme.

ABSTRACT

TARGETED DELIVERY OF ATORVASTATIN BY APTAMER GATED SILICA NANOPARTICLES IN ATHEROSCLEROSIS CELL CULTURE MODEL

Cardiovascular diseases (CVD) are the number one cause of deaths all around the world in which atherosclerotic CVD have the biggest portion. Atherosclerosis, known as a chronic inflammation at arterial wall, is caused by endothelial cell (EC) dysfunction which is reported to be induced by low shear stress. In addition, atorvastatin is one of the most commonly used drug in the treatment of atherosclerosis. Targeted delivery of atorvastatin to the atherosclerotic area could increase the efficacy of the drug and minimize the side effects of atorvastatin including adverse muscle events and hepatic dysfunction. Aptamers are single stranded DNA or RNA sequences which have unique tertiary structures that enable them to bind a specific protein of interest. In the present study, aptamers were designed to target intracellular adhesion molecule-1 (ICAM-1) which is an inflammatory marker and increased in atherosclerotic area. In addition, aptamer gated atorvastatin loaded silica nanoparticles (APT-ATS-NP) used in the present study provides controlled release of the atorvastatin. Therefore, the aim of the present study was to research targeted delivery and controlled release of atorvastatin by APT-ATS-NP under normal and low shear stress conditions in the human umbilical vein endothelial cell (HUVECs), which mimics healthy and atherosclerotic conditions, respectively. HUVECs were incubated with different concentrations of atorvastatin which was delivered by APT-ATS-NP under low oscillatory conditions (2.63 dyn/cm^2) for 24 hours. In order to evaluate the effects of APT-ATS-NP, intracellular ROS levels were measured by using flow cytometry and protein expression levels of eNOS, Akt, peNOS, pAkt were measured by western blot. Intracellular ROS levels were significantly reduced by 0.1 mM atorvastatin delivery by APT-ATS-NP. Moreover, 5 nM atorvastatin delivery by APT-ATS-NP increased the phosphorylation levels of Akt and eNOS proteins. Therefore, application of aptamer gated nanoparticles in the treatment of atherosclerosis by atorvastatin could be more effective in clinical practices.

ÖZET

ATEROSKLEROZ KOŞULLARINDA HÜCRE KÜLTÜRÜ MODELİNDE APTAMER VALFLİ SİLİKA NANOPARÇACIKLARLA HEDEFE YÖNELİK ATORVASTATİN TAŞINMASI

Kardiyovasküler hastalıklar en yaygın ölüm sebebi olarak kabul edilmektedir ve aterosklerotik kalp hastalıkları bu hastalıklar içinde en büyük paya sahiptirler. Ateroskleroz, endotel hücrelerin disfonksiyonu nedeniyle damar çeperlerinde kronik inflamasyon oluşmasıyla tanımlanmaktadır ve düşük kayma geriliminin bu durumu tetiklediği bulunmuştur. Bu bağlamda, atorvasatin ateroskleroz tedavisinde en yaygın olarak kullanılan ilaçtır. Atorvastatinin hedefe yönelik olarak taşınması ilacın hepatik disfonksiyon ve kas harabiyeti gibi yan etkilerini azaltabilir ve ilacın etkinliğini arttırabilir. Aptamerler, özgün tersiyer yapıları sayesinde spesifik olarak belirlenmiş bir proteini hedefleyebilen tek zincirli DNA veya RNA dizileridir. Bu çalışmada, aterosklerotik bölgelerde arttığını bilinen inflamatuar bir marker olan hücre içi adezyon molekülü-1'i (ICAM-1) hedefleyen aptamer kullanılmıştır. Ek olarak, bu çalışmada kullanılan aptamer valfli atorvastatin yüklü silika nanoparçacıklarla (APT-ATS-NP) ilacın kontrollü salınımını sağlamaktadır. Bu sebeple, bu çalışmada HUVEC hücreleri APT-ATS-NP aracılığıyla veya direkt uygulanan atorvastatin ile 24 saat boyunca normal ve düşük kayma gerilmesine maruz bırakılmıştır, bu uygulamayla sağlıklı ve ateroskleroz koşullarını modellemektedir. HUVEC hücreleri düşük salınımlı akış koşulları (2.63 dyn/cm^2) altında APT-ATS-NP aracılığıyla taşınan farklı atorvastatin konsantrasyonlarıyla inkübe edilmiştir. APT-ATS-NP'nin etkisini belirlemek amacıyla hücre içi serbest radikal miktarı (ROS) akış sitometrisi ile ölçülmüştür ve eNOS, Akt, peNOS, pAkt protein seviyeleri western blot ile ölçülmüştür. 0.1 mM atorvastatin APT-ATS-NP ile uygulandığında, direkt uygulamaya göre ROS seviyesini istatistiksel olarak anlamlı şekilde azaltmıştır. Ayrıca, APT-ATS-NP ile 5 nM atorvastatin uygulanması Akt ve eNOS proteinlerinin fosforillenme seviyeleri direkt atorvastatin uygulanmasına göre artmıştır. Bu bağlamda, bu çalışmada kullanılan aptamer valfli atorvastatin yüklü nanoparçacıklar, atorvastatin ile ateroskleroz tedavisinin klinik uygulamalarında daha etkin olabilir.

TABLE OF CONTENTS

LIST OF FIGURES

LIST OF TABLES

LIST OF SYMBOLS/ABBREVIATIONS

μM	micro molar
nM	nano molar
μl	microliter
3-hydroxy-3-methylglutaryl-coenzyme-A	HMG-CoA
AMP-activated protein kinase	AMPK
atorvastatin loaded aptamer gated silica nanoparticles	APT-ATS-NP
cardiovascular disease	CVD
cyclic guanosine monophosphate	cGMP
Endothelial nitric oxide synthase	eNOS
extracellular matrix	ECM
High-density lipoproteins	HDL
human umbilical vein endothelial cell	HUVEC
insulin-like growth factor 1	IGF-1
intracellular adhesion molecule-1	ICAM-1
Low-Density Lipoprotein	LDL
nitric oxide	NO
phosphorylated AKT	pAkt
phosphorylated eNOS	peNOS
protein kinase A	PKA
protein kinase B	Akt
reactive oxygen species	ROS
smooth muscle cells	SMC
statin-associated muscle symptoms	SAMS
vascular adhesion molecule-1	VCAM-1
vascular endothelial growth factor	VEGF
Very low-density lipoproteins	VLDL

1. INTRODUCTION

Atherosclerosis is a common cardiovascular disease and preventive treatment of atherosclerosis in early stages are very important. In this context, we targeted inflammation in the present study since it is an initiative step of pre-atherosclerosis. Therefore, ICAM-1, an inflammatory biomarker, was targeted by aptamer gated nanoparticles (APT-ATS-NP) for atorvastatin delivery to human umbilical vein endothelial cells (HUVECs) which were exposed to low shear stress for mimicking pre-atherosclerosis conditions during the experiments. The effects of atorvastatin delivery by APT-ATS-NP was evaluated by measuring intracellular ROS levels and phosphorylation levels of Akt/eNOS proteins.

1.1. ATHEROSCLEROSIS

Atherosclerosis is a chronic inflammatory disease of the arterial wall which causes the accumulation of lipids and fibrous material in the area. Atherosclerotic cardiovascular diseases (ACVD) involve ischemic heart diseases such as myocardial infarction and stroke which have the biggest portion of cardiovascular diseases (CVD) related deaths worldwide [1]. In North Africa and the Middle East, CVD is the reason for thirty-nine percent of all deaths [2]. According to the report Global Burden of Diseases, Injuries, and Risk Factor Study, there were 7.29 million acute myocardial infarctions in 2015 and studies revealed that %75 of myocardial infarction is caused by late-stage atherosclerosis. The same study indicated that 6.33 million deaths were caused by stroke. Overall %31 global deaths were caused by CVD, with ACVD occupying the biggest portion, in 2015.–Despite the improvement in treatments, atherosclerosis is still very common in developed nations, and the prevalence rate in developing countries is very concerning. In 2012, the CVD-related deaths were recorded as 17.5 million, in 2016 this number was 17.9 million and the expected number for 2030 is around 22.2 million (WHO, **2016**, **2017**) [3–5].

Atherosclerosis is a condition that affects large and medium-sized arteries in almost all humans. Even though it starts to form in childhood it becomes detectable by aging. With the increase in the western-type diet, cholesterol-rich food, less active lifestyle, and unhealthy habits such as smoking the prevalence of atherosclerosis increases. Atherosclerosis is initiated by the accumulation of fibrous and lipid material, which forms *atheroma*s or

atherosclerotic plaques in the arterial wall. These plaques may calcify and over time they may cause narrowing of the lumen, *stenosis*, or in another way, they may rupture and cause the formation of thrombi. Atherosclerosis may lead to several life-threatening diseases since narrowing of the vessel may cause ischemia of the vital organs depending on the localization of plaque, and thrombi may cause stroke or myocardial infarction.

1.1.1. Blood Vessels and Layers

Atherosclerosis is a disease that occurs at vessel walls, therefore it is important to understand the structure. Blood vessels are structured with layers. The outside layer of the vessel "*adventitia*" consists of connective tissue and nerve fibers to cover the "*media*" layer which has smooth muscle cells and an extracellular matrix (ECM). The thickness of these layers can vary between vessel types. Arteries have thicker adventitia and smooth muscle cells (SMC) rich media to accommodate high blood pressure and pulsatile flow. On the other hand, veins are capable to carry a higher volume of blood and have thinner walls because of low blood pressure. *Internal elastic lamina* separates media from the "*intima*" layer, which is the inner layer and barrier between blood and vessel. Intima consists of endothelial cells, a specific type of epithelial cell, and a minimal extracellular matrix [1]. (Figure 1.1)

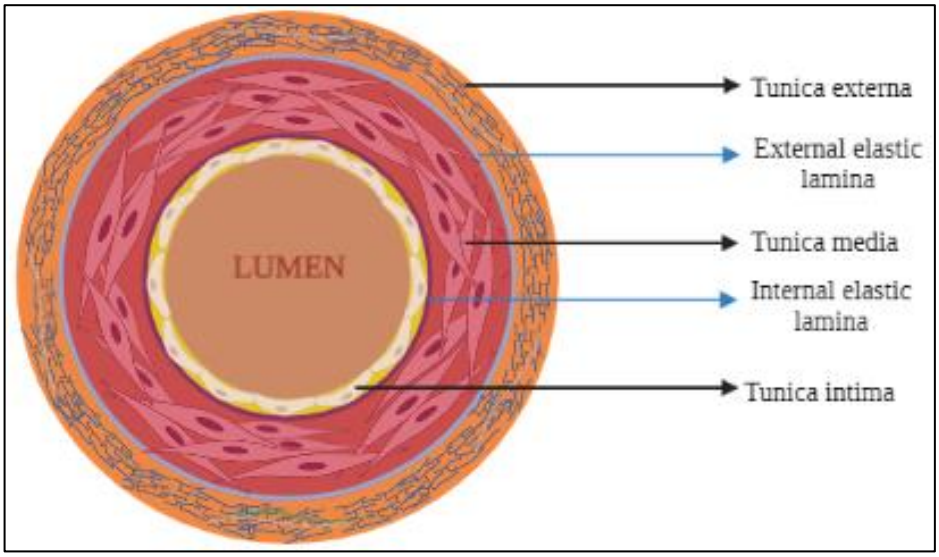

Figure 1.1. Blood Vessel Layers

1.1.2. Endothelial Cells Function and Dysfunction

The pathogenesis of atherosclerosis is explained by the response to injury hypothesis. In this aspect, atherosclerosis is defined as a chronic inflammatory response of the arterial wall caused by endothelial injury. Disturbed blood flow, hypertension, hyperlipidemia, cytokines, and/or hypoxia are common causes of endothelial dysfunction [1]. Disturbed flow and subsequent change of shear stress will be discussed in the next chapter.

Endothelial cells have several functions apart from being a permeable barrier. Non-thrombogenic feature of the blood-tissue interface is provided by the anticoagulant, anti-thrombotic and fibrinolytic regulators that are secreted by ECs. The factors needed to regulate blood flow and vascular tone are produced by ECs. In addition, ECs take place in inflammatory response and immunity by presenting several adhesion molecules such as intracellular adhesion molecule-1 (ICAM-1), and vascular adhesion molecule-1 (VCAM-1) for leukocytes and secreting cytokines [6,7].

Endothelial activation or endothelial dysfunction causes increased expression of pro-coagulants, adhesion molecules, and pro-inflammatory cytokines. In addition, change in chemokine, cytokine, and growth factors expression occurs. Endothelial activation may be caused by turbulent blood flow, hypertension, cytokines, hyperlipidemia, hypoxia, viruses, and bacterial products. Vascular wall responses to endothelial injury by several processes. Firstly, ECs loss or injury triggers SMC growth and migration which accumulates in the intima layer where they produce new ECM components such as collagen and fibrinogen. However, this migrated SMC does not have contractility. Migration and activation of SMCs regulated by growth factors such as insulin-like growth factor 1 (IGF-1), cytokines produced by platelets and ECs, macrophages, coagulation, and complement factors. In the case of normalization in the EC layer, intimal SMC becomes non-proliferative. Gradual ongoing thickening was evaluated as a consequence of “normal aging”. Fortunately, outward remodeling on the vessel causes little change in diameter [1].

However, when the “activation” of ECs is constant they do not maintain their function in balance which is the initial step of atherosclerosis. Decreased eNOS levels and phosphorylation and increased ROS levels are important steps of endothelial dysfunction which were discussed in the sections below in more detail.

1.1.3. Shear Stress

Shear stress is defined as the ratio of tangential frictional force caused by blood flow to the surface area. Shear stress of large arteries, such as the aorta, is found to be 6 dyn/cm^2 up to 20 dyn/cm^2, on the other hand, low shear stress which is observed in atherosclerotic regions is smaller than 4 dyn/cm^2 [8,9]. Endothelial cells modify their activity by mechanical sensing of shear stress. There are several pathways suggested for taking part in the induction of ECs by SS [10]. (Figure 1.2)

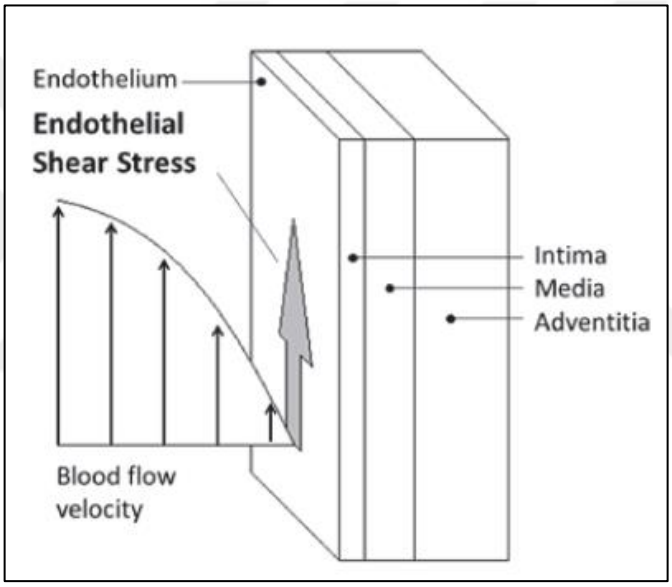

Figure 1.2. Schematic representation of endothelial shear stress. [11]

Mechanotransducers are one of the suggested sensors that are able to transduce the mechanical stimuli into a biological process such as phosphorylation. The most common sensors in the literature are primary cilia and glycocalyx which is a carbohydrate-rich layer lining the endothelium. In addition, ion channels, integrins, receptor tyrosine kinases, platelet-endothelial-cell adhesion molecule-1 (PECAM-1), and vascular endothelial cadherin (VE-cadherin) are considered potential mechanical sensors [10,12]. Another model for mechanical sensing is tensional integrity [13]. In this model, the cell is considered as a shape that is maintained by the cytoskeleton and this structure is ensured by tensional pre-stress. In the presence of a mechanical change, the forces on the tensional integrity are

modified. Subsequently, several biochemical reactions are initiated by these changes. [10,14].

In blood vessels, two main flow form is observed; laminar and oscillatory (turbulent) flow. Laminar flow (10-20 dyn/cm^2) maintains ECs function and atheroprotective state by promoting anti-coagulant factors, decreasing inflammation, reducing smooth muscle cell proliferation, and increasing EC survival [15].

Even though the systemic risk factors are equally distributed through the vasculature, atherosclerotic plaques are generally located on the sites where blood flow is disturbed which causes low shear stress. Wall shear stress is related to the velocity of blood flow and viscosity of blood. The balance of centrifugal, pressure and viscous forces are not equally distributed asymmetric profiles are observed in bending arteries and bifurcation regions where separation of flow can occur and cause oscillating flow. In conclusion, this distinct distribution causes low and high shear stress areas at the vessel wall. Low shear stress and subsequently plaque formation are observed at branching points of the vessel, the outer waist of bifurcations, or the inner curve of arteries [11].

One of the most important early markers of atherogenesis is the adherence of immune cells to ECs. Therefore, the regulation of local inflammation in atherosclerosis is dependent on the elevation of adhesion molecules like ICAM-1 on the endothelium of blood arteries [16]. Studies revealed that shear stress acting on ECs affects the expression of ICAM-1. In the paper of Nagel *et al.*, HUVECs were exposed to 3 or 10 dyn/cm^2 shear stress, and a significant increase of ICAM-1 level was obtained starting from 8 hours [17]. In another study with HUVECs, exposure to 25 dyn/cm^2 shear stress for 12 hours increased the surface expression of ICAM-1. Combining the effect of inflammatory stimuli (TNF-α treatment) and shear stress showed that 20 dyn/cm^2 shear stress caused an increase in the TNF-α–induced expression of ICAM-1 of the ECs. In one study with human coronary artery ECs, 5-12 dyn/cm^2 was referred to as normal physiological shear stress and 0.1-3 dyn/cm^2 was referred to as low. Shear stress in this study was applied with pulsatility. The results indicated that low pulsatile shear stress had significantly higher levels of ICAM-1 mRNA and protein [18]. In this context, ICAM-1 targeted drug delivery for treatment of atherosclerosis provides an advantage to achieve treatment in pre-atherosclerosis stage and as a result preventing the development of atherosclerosis in advance. Therefore, in the present study HUVECs were exposed to LOF, and the target of the drug delivery system was determined as ICAM-1.

1.1.4. Low-Density Lipoprotein (LDL) Infiltration and Oxidization

The primary event in the formation of atherosclerosis is the infiltration of LDLs into the subendothelial space. After infiltration LDLs are oxidized and this process activates ECs to increase the expression of cell adhesion molecules, and recruitment of leukocytes and monocyte to the region.

LDLs are carriers of cholesterol through the body because of the hydrophobic nature of cholesterol and tryacyl glycerol (TGA) transported via lipoproteins. LDLs contain approximately 1500 cholesterol molecules within. In the core of LDL, esterified cholesterols are found and they are surrounded by phospholipids and unesterified cholesterol. This shell also contains apolipoprotein B-100 which is recognized by the target cell and also solubilizes hydrophobic lipids. Apart from the transport of cholesterol to peripheral tissues, LDL regulates de novo cholesterol synthesis.

Cholesterol is a fundamental component of cell membranes and is the precursor of steroid hormones such as progesterone, testosterone, and estradiol. Several lipoproteins differ in function, size, and cholesterol ratio. Chylomicrons take place in dietary fat transport and have a 75-1200 nm diameter. Very low-density lipoproteins (VLDL) function in endogenous cholesterol transport and has a higher size and lipid/protein ratio compared to LDL. Excess TGA and cholesterol are released into the blood from the liver where they are produced in VLDL. On the capillary surfaces lipases, an enzyme family functions in hydrolyzing lipids, are found and VLDLs are hydrolyzed by them. The rest of the VLDL contains a cholesterol-ester-rich remnant and is referred to as intermediate-density lipoprotein (IDL). Approximately half of the IHL is taken up by the liver for processing and the other half is converted to LDL by removal of more TGA by tissue lipases that absorb released fatty acids. High-density lipoproteins (HDL) are around 7.5-20 nm and function in the uptake of cholesterol which is released by dying cells to plasma or from membranes undergoing turnover. Later on, HDL delivers the cholesterol to the liver for excretion because the steroid nucleus cannot be degraded by cells.

Increased plasma LDL level is one of the major factors of atherosclerosis pathogenesis. The first evidence of this hypothesis is provided by patients with homozygous familial hypercholesterolemia (FH) since they develop atherosclerosis and had a myocardial

infarction in the first two decades of their life. Even though homozygous FH patients have no LDL-R or they have a few, accumulation of LDL in arterial lesions and subcutaneous tissue is observed. This information proved that the accumulation of cholesterol is maintained by another pathway rather than LDL-R.

LDL oxidization occurs by several stimuli including metals, hemoglobin, and reactive oxygen species (ROS) from vascular cells or mitochondria. Malondialdehyde (MDA) is one of the most common oxidative agents for lipid peroxidation and one of its substrates is LDL. Therefore, MDA-LDL complexes were found to be present in the progression of atherosclerosis [19].

Oxidized or modified LDL is engulfed by macrophages by several mechanisms, except for LDL-R, and accumulates in the arterial wall. These receptors are referred to as acetyl LDL receptors and they have been reported to be not affected by the increased intracellular LDL levels, unlike the LDL-R amount which is decreased by LDL elevation in the cell as a feedback mechanism. After the isolation and characterization of the acetyl LDL receptor, it is designated as scavenger receptor, type A or SR-A. However, further studies showed there are non-scavenger receptors that take place in the uptake of LDL by macrophages. Studies showed that macrophages are not able to engulf LDLs when they are in their native form which showed oxidation of LDL is a promoter of LDL atherogenicity and subsequently atherosclerosis [19].

1.1.5. Decreased NO bioavailability

The abnormal change in ECs is often caused by the imbalance of endothelial factors, such as nitric oxide (NO), a multifunctioning signaling molecule. NO is well-known for its vasodilator function, however, it also regulates gene transcription, mRNA translation (by binding to iron-responsive elements), and post-transcriptional modification of proteins [20]. Decreased NO availability is a pivotal cause of atherosclerosis. Reduction in NO level may be the consequence of ox-LDL formation, oxidative stress, or inflammation in the area [21].

Endothelial nitric oxide synthase (eNOS) (explained in the next chapter) dependent NO has a fundamental role in the dilation of all blood vessels via the cyclic guanosine monophosphate (cGMP) pathway in SMCs [22]. In this reaction binding of NO to the heme

moiety of soluble guanylyl cyclase (sGC) activates this enzyme up to 200-fold [23,24]. sGC catalyzes the conversion of GTP to cGMP. cGMP maintains its SMC relaxing function mainly through cGMP-dependent protein kinases (PKG). PKG is activated by binding to cGMP and active PKG phosphorylates key proteins that are involved in the reduction of intracellular Ca^{2+} concentration. For example, PKG may directly inhibit Ca2+ channel activity or activates Ca^{2+}-activated K^{+} channels (KCa) and this activation subsequently causes a reduction of Ca^{2+} influx and hyperpolarizes the cell membrane which leads to SMC relaxation. Inositol triphosphate (IP3) receptors are another substrate of PKG. Phosphorylation of IP3 receptors decreases its channel activity at the sarcoplasmic reticulum and causes a reduction of Ca^{2+} efflux resulting in SMC relaxation [22,23]. Apart from these mechanisms, cGMP might reduce the sensitivity against Ca^{2+} in the contractile system [23].

Apart from its effect on the relaxation of SMCs, NO may also inhibit the proliferation of SMCs by the cGMP pathway. The proliferation of SMCs is a fundamental step in atherogenesis therefore presence of NO has a protective role against atherosclerosis [20,25].

ECs are important modulators of pro-inflammatory response. Endothelial NO has a protective role against apoptosis of ECs by pro-inflammatory cytokines and reactive oxygen species (ROS). In addition, NO modulates leucocyte adherence to the ECs which is a fundamental step in the start of atherosclerosis. Thereby, decreased bioavailability of NO can initiate atherosclerosis [20].

1.1.5.1. Roles of eNOS in atherosclerosis

Approximately 40 years ago Furchgott and Zawadski reported that ECs produce a factor that has a role in the relaxation of underlying VSMCs and in 1996 Murad, Furchgott, and Ignarro were rewarded by Nobel Prize for their discovery that NO is an essential regulator of vasodilation. However, nitric oxide synthase (NOS) enzymes were characterized previously and the structure of the enzyme had already been known [26,27]. NOS enzyme has 3 subtypes : endothelial NOS (eNOS), inducible NOS (iNOS), and neuronal NOS (nNOS) [28,29]. All of the subtypes of NOS require cofactors: reduced nicotinamide-adenine-dinucleotide phosphate (NADPH), flavin adenine dinucleotide (FAD), flavin mononucleotide (FMN), and (6R-)5,6,7,8-tetrahydrobiopterin (BH4) [20]. In addition, all subtypes of NOS contain calmodulin-binding sequence and haem in their structure.

nNOS is abundant in specific neurons where it might be in particulate or soluble form. The function of nNOS includes long-term regulation of synaptic transmission [30], central regulation of blood pressure [31], regulation of vascular tone in the periphery [32], and penile erection [33]. Interestingly smooth muscle cells were reported to express nNOS in case of predominant eNOS is dysfunctional [34]. iNOS is expressed in several cell types such as macrophages and its expression is dependent on stimuli such as bacterial lipopolysaccharides, and cytokines [32,34]. However, when iNOS is expressed it presents in active form constantly and can synthesize toxic levels of NO inside the cells, especially in macrophages [35]. A high level of NO causes inhibition of enzymes that contain iron in their enzymatically active region due to the high affinity of NO to protein-bound iron [35]. In addition, a high level of NO in macrophages directly damages the DNA of target cells and causes cytotoxicity [36]. In addition, iNOS is involved in non-specific allograft rejection and septic shock [37,38].

eNOS is abundant in ECs, however, the enzyme is also expressed in myocytes, platelets, specific neurons of the brain, and kidney epithelial cells [20,34].

eNOS contains two domains; the N-terminal oxygenase domain contains binding sites for haem, BH_4, and L-arginine, C-terminal reductase domain includes FAD, FMN, and NADPH binding sites. Calmodulin recognition site connects oxygenase and reductase domain [39] (Figure 1.3).

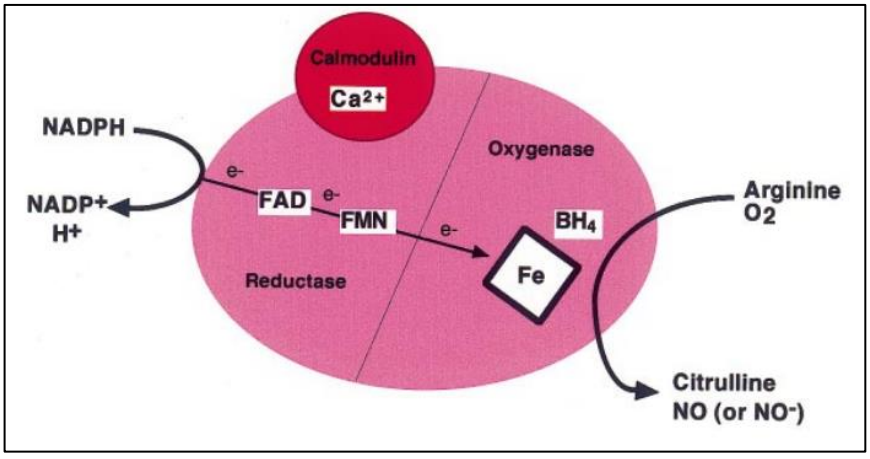

Figure 1.3. Schematic structure and subdomains of eNOS [34]

Most of the NO is synthesized by endothelial cells in the body [40]. L-arginine is the substrate of all NOS enzymes for NO synthesis. In the enzymatic reaction, NOS transfers electrons from NADPH, via FAD and FMN, to the haem in the oxygenase domain which is the part of the NOS that contains BH_4. At the haem part, L-arginine is oxidized by reduction and activation of O_2 to produce L-citrulline and NO [20].

eNOS functions in the homodimer form, in fact, studies previously reported that the uncoupling of eNOS is a fundamental cause of endothelial dysfunction in atherosclerosis [41,42]. Phosphorylation of serine 1177 (Ser-1177) is critical for activation of eNOS [43,44]. Ser-1177 located at the carboxyl-terminal tail of eNOS is "wedged" between monomers and therefore inhibits electron transfer among monomers. Phosphorylation of this site creates a conformational change that removes the wedge and allows the formation of eNOS homodimer and increases eNOS activity [45,46].

eNOS is phosphorylated according to several stimuli. For example, Ox-LDL restrains phosphorylation of Ser-1177, therefore, attenuating eNOS activity and decreasing NO bioavailability [47,48].

In the study of Dixit *et al.,* ECs are exposed to the shear stress of 12 dyn/cm^2 after that phosphorylation and activation of Akt and eNOS are observed. Laminar shear stress is shown to increase phosphorylation of eNOS at Ser1177 residue by both Ca2+/calmodulin dependent kinase II and Akt pathway dependent on the rate of change in shear stress between 1.8-25 dyn/cm^2 [49,50]. Overall, hemodynamic factors regulate vasculature by shifting endothelial cell physiology.

1.1.5.2. Roles of Akt in atherosclerosis

The kinases catalyze the phosphorylation of eNOS, such as protein kinase B (Akt), protein kinase A (PKA), AMP-activated protein kinase (AMPK), and calmodulin/Ca2+ dependent protein kinase (CaMKII) [46].

Akt, which is a serine/threonine kinase, is one of the most studied kinases in the eNOS phosphorylation pathway [51,52]. The effect of Akt on eNOS activation has been reported in several studies. For example in one study with COS-7 cells (which do not express NOS), it was reported that NO levels and phosphorylation of eNOS were increased in case of co-transfection of eNOS with wild-type Akt, but this effect was not observed with kinase-inactive Akt. In addition, mutation of serine 1179 (serine 1177 in humans) abolished

phosphorylation of eNOS by Akt [52]. These results indicate that Akt modulates NO production by activating eNOS at Ser-1179 (Ser-1177) site [52]. Studies show that Akt is activated by phosphorylation, creates phosphorylated AKT (pAKT), under mechanical forces such as shear stress, and after it is activated it can phosphorylate its substrates [52]. The phosphoinositide 3-kinase (PI3K) pathway is one of the mechanisms that phosphorylates and therefore activates AKT. For example in the study of Dimmeler et al. 15 dyne/cm^2 shear stress was applied to HUVECs and it has been reported that Akt phosphorylation was increased in a time-dependent manner by shear stress [53]. In another study, exposure to 12 dyne/cm^2 shear stress on HUVECs for an hour resulted in a two-fold increase in phosphorylation of serine residues of eNOS, and incubation with Akt phosphorylation inhibitor reversed the shear stress-inducing phosphorylation of eNOS [54]. The same study reported that mutation of Ser-1177 reduced the phosphorylation of eNOS by Akt stimulated by shear stress. In conclusion, these studies prove that eNOS is a substrate of Akt, and stimulation of Akt by shear stress enhances eNOS activity by phosphorylation of serine residues [54].

1.1.6. Increased Production of Reactive Oxygen Species (ROS)

Oxidative stress, the imbalance between ROS production and the innate anti-oxidant system of the body, is a driving force in the pathogenesis of many diseases including CVD. Oxidization of lipids and proteins has been reported in the studies with vascular lesions and it has been elucidated that oxidative stress and severity of the disease have a positive correlation [55]. Disturbed flow induces ROS production in ECs and VSMCs [56]. ROS are produced in the vasculature by several systems including NADPH oxidase (Nox), xanthine oxidase (XO), enzymes of the mitochondrial respiratory chain, and uncoupled endothelial NO synthase [25,57].

It has been reported that deletion of Nox1, an isoform of Nox, resulted in a reduction in atherosclerosis in apolipoprotein-E deficient mice fed with an atherogenic diet [58]. In another study, overexpression of Nox2 was reported to increase processes related to the pathogenesis of atherosclerosis including vascular superoxide production, endothelial vascular cell adhesion molecule-1 expression, and recruitment of inflammatory cells [59]. The essential role of Nox in LDL oxidation in macrophages/monocytes has been evaluated

in another study [60]. Increased XO activity has been found in atherosclerosis models and human atherosclerotic plaques and inhibition of XO reduce the development of atherosclerosis in mice models [61–64]. Heterozygous mitochondrial superoxide dismutase (SOD) knockout atherosclerotic mice were reported to have increased ROS and atherogenesis compared to wild type [65]. As indicated in the previous section eNOS has a protective role against atherosclerosis, however, under oxidative stress, it is in uncoupled form and produces superoxide which has been evaluated in mouse models of atherosclerosis [66,67]. Scavenger receptors (SR) are found in the membrane of macrophages and they internalize modified lipoproteins such as ox-LDL. ROS increases the SR levels in SMC which facilitates the formation of atherosclerotic plaques [68].

NO and free radicals may react and form peroxynitrite ($ONOO^-$), which is not protective against atherosclerosis. In contrast, peroxynitrite contributes formation of atherosclerosis by modifying lipids and proteins, such as the formation of ox-LDL, and increases vascular inflammation. Therefore, increased ROS causes a decrease NO bioavailability which is an accelerating mechanism in the formation of plaques [56,69].

Finally, oxidative stress is a pivotal contributor to the pathogenesis of atherosclerosis, therefore therapeutic strategies that target ROS generation, such as statins, may reduce oxidative stress and contribute to achieving an atheroprotective state.

1.1.7. Atherosclerotic Plaque Formation and Progression

The pathology of atherosclerosis is characterized by chronic inflammation of the blood vessels. These sites are generally located at branching points of vessels where the blood flow is disturbed which is a reason for endothelial dysfunction and structural alteration such as decreased elastin amount. Endothelial dysfunction might be triggered by several reasons for example; hypertension, hyperlipidemia, toxins from cigarette smoke, or viruses. Endothelial dysfunction permits infiltration of LDLs (via SRs) and monocytes inside the intima layer due to increased permeability and increased adhesion molecule expression such as ICAM-1 and VCAM-1. LDLs are oxidized in the intima layer since they are susceptible to oxidative modification by ROS. Ox-LDLs are recognized and engulfed by macrophages and this process turns them into foam cells. Foam cells start inducing the secretion of adhesion molecules, chemokines. As indicated in previous chapters, decreased NO bioavailability,

increased ROS, and changes in the transcription of several genes and protein expression are important contributors to lesion formation by several pathways [1,70] (Figure 1.4).

A pro-inflammatory state triggers intimal immune cell infiltration. T cells are recruited and activated inside the intima layer where they secrete inflammatory cytokines such as interferon-γ, interleukin-1, and monocyte chemoattractant protein 1 (MCP-1) which again triggers macrophages, ECs, and SMCs in the growing intimal lesions and facilitate infiltration of inflammatory cells. Fatty streaks are the early lesions that are composed of T-cells and foam cells and do not cause any significant flow disturbance. Chronic inflammation results in the release of growth factors by inflammatory cells and vascular wall cells that induces SMC migration to the intima layer and ECM component synthesis. This change converts fatty streaks into atheromas or atherosclerotic plaques which have a range of 0.3 to 1.5 cm in diameter, are white to yellow, patchy, and characterized by intimal thickening and lipid accumulation. Later stages may involve calcification and SMC death might be observed which results in a relatively acellular core, the necrotic core that contains dying or dead cells. Generally, plaques have a fibrous cap that contains SMCs and collagen and cover the necrotic core that contains lipids, SMCs, foam cells, necrotic debris, and plasma proteins. The lesion is nurtured by the formation of new blood vessels, which is a process referred to as neovascularization [1,71].

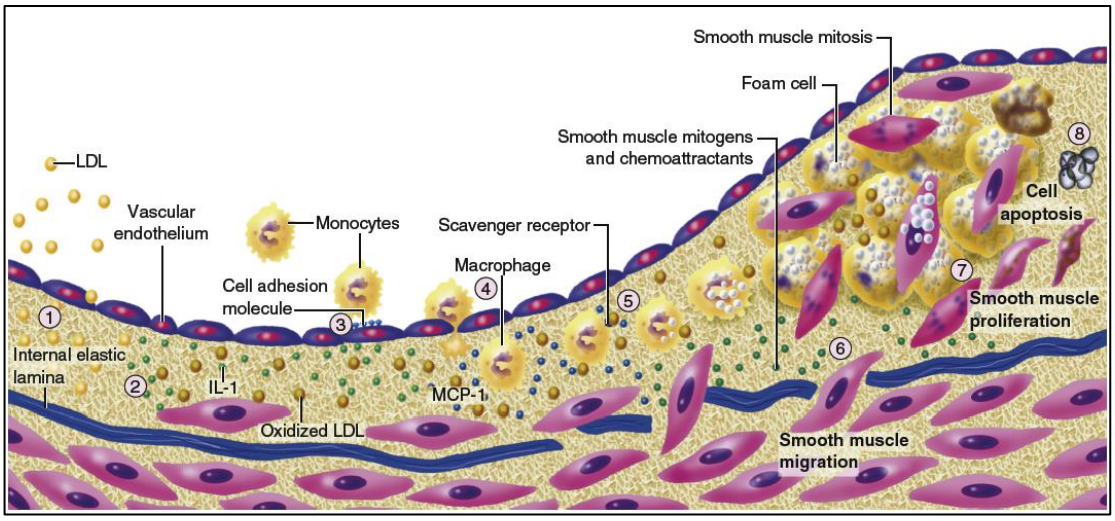

Figure 1.4. Atherosclerotic plaque formation [71]

Clinically there are a few steps that the plaques are susceptible to. The plaque may go under rupture, ulceration, or erosion which triggers the thrombogenic process and results in

thrombus formation. Thrombus has the potential to partially or completely occlude the lumen and therefore causing to tissue ischemia (e.g., in the heart). Rupture of the fibrous cap on the thin-walled vessels may cause intra-plaque hemorrhage and may cause rapid plaque growth. On the other hand, rupture may cause microemboli due to the discharge of debris into the blood. The pressure of the atherosclerotic area or ischemic atrophy and loss of elasticity may cause the formation of an aneurysm. Another consequence of plaque growth is critical stenosis, which is defined as chronic occlusion that limits the flow so severely that tissue demands are not supplied [1,71].

Atherosclerosis-related CVDs create an enormous burden on the healthcare system due to the high incidence rate. Currently, the therapeutic perspective is optimistic due to the encouragement of healthy lifestyle choices, better therapeutic strategies by the new biomarker, and genetic research. In addition, as indicated above atherosclerosis progression occurs step by step which provides an advantage to prevent progression of the disease by targeting the mechanisms in the progression steps. For example targeting inflammation for the treatment of atherosclerosis demonstrates an advantage by targeting pre-atherosclerosis step and subsequently may contribute to better treatment [71].

However, the most common treatments for the prevention of atherosclerosis are reducing hypertension, controlling hemostasis for the prevention of thrombosis, and most commonly lowering the blood lipids. Therefore, statins, highly effective LDL lowering drugs, are the most common drugs in clinical usage for atherosclerosis treatment [70,72].

1.2. STATINS

Statins are a synthetic reversible competitive inhibitor of 3-hydroxy-3-methylglutaryl-coenzyme-A (HMG-CoA) reductase. Statins manage their most common function, lipid-lowering, by inhibition of HMG-CoA, the rate-limiting enzyme of hepatic cholesterol production which is referred to as the mevalonate pathway [73].

Statins are firstly discovered in the early 1970s by Dr. Akira Endo in molds like fungi and mushrooms. Back then a series of compounds were found by Endo and they were described by their antibacterial activity due to inhibition of cholesterol biosynthesis. First studies with rodents resulted in low antibacterial activity and ineffectiveness for cholesterolemia.

However, the studies with human cells gave rise to this exciting area of therapy. Studies of Goldstein and Brown with human fibroblasts and adrenal cells indicated that statins cause upregulation of HMG CoA reductase. This result proved that the synthesis of the enzyme was regulated via a constant feedback mechanism by cholesterol, therefore statin, compactin was the name of the product in that study, release that repression. On the other hand, LDL-R was regulated by the same feedback mechanism and studies reported that statins induced an increase in LDL-receptor activity in cultured fibroblasts, adrenal cells, and whole animal liver. As a result of these promising results, there was an increase in statin studies. In 1987, Merck commercialized lovastatin [74,75]. The success of statins was first investigated with familial hypercholesterolemia patients, the study resulted in decreased cholesterol levels. However, adverse effects such as elevation of transaminases and muscular dystrophy were reported. The Scandinavian Simvastatin Study was a large-scale randomized trial and it evaluated that simvastatin treatment resulted in a 25% reduction in total plasma cholesterol and a 35% decrease in LDL in patients with coronary heart disease or myocardial infarction history [76].

Statins can be classified according to their source, fungal-derived; lovastatin, pravastatin, and simvastatin, or synthetically produced; atorvastatin, cerivastatin, fluvastatin, pravastatin, pitavastatin, and rosuvastatin. Natural and synthetic statins differ in the context of function due to their hydrophobicity and ability to interact and inhibit HMG-CoA reductase. The affinity of the HMG-CoA for statins is approximately 8000 fold higher compared to its natural substrate, HMG-CoA, this information shows the importance of statins. Synthetic statins form more interaction with the enzyme due to their structural characteristics [77,78].

Statins are well-tolerated drugs in general, however, some adverse effects were recorded in the long-term trials. Hepatotoxicity is one of the most common adverse effects of statins. Elevation of liver enzymes to three-fold was reported with dose-dependent atorvastatin administration in 3% of the patients. The increase of transaminases in the serum was related to hepatocyte membrane alteration due to treatment, rather than the direct injury of the liver. UK Committee on Safety of Medicines (CSM) reported four deaths due to hepatic diseases which are associated with atorvastatin treatment. It has been evaluated that hepatic adverse effects mostly occurred in over 60 years female patients [79,80]. Another side effect of statin treatment is myopathy, which is defined as aching muscles or and disease affecting voluntary muscle movement. These conditions are also referred to as statin-associated muscle

symptoms (SAMS). SAMS was reported in 10-29% of the patients in observational studies. However, only 0.2% of patients under statin treatment have been reported to have ten times higher creatine phosphokinase levels than normal which is a marker of injury or stress of muscles. Rhabdomyolysis is one of the worse consequences of myopathy which is a process that involves the breakdown of muscle tissue and the release of muscle fiber contents into the blood. 0.1% of the patients under statin therapy had rhabdomyolysis and acute renal failure. Fortunately, reduction of statin dosage or drug discontinuation was able to stop these side effects [79,81]. In the literature, it has been underlined that even though there is a higher rate of SAMS, the occurrence of myopathy is rare. There are other side effects observed with statin treatment related to the gastrointestinal tract such as nausea, constipation, diarrhea, or bloating. Those effects are generally lost spontaneously in 2-3 weeks. Large trials of statins have a long history and early study designs did not include type-2 diabetes as a clinical end point due to clinical irrelevance. In 2008, a large-scale study with rosuvastatin revealed a 25% increase in newly diagnosed diabetes compared to the placebo control group. However, subsequent analysis of that study reported that the beneficial effects of drug on cardiovascular events exceeds the risk of diabetes. In another study with 80 mg atorvastatin treatment, 44% increase in early-onset diabetes was observed in patients with prior stroke or transient ischemic attack, this results suggests a dose-dependent effect. Analysis of five large scale trials demonstrated that intensive statin therapy results in 12% higher diabetes risk compared to less-intensive statin therapy. The relation of statin and diabetes progression is suggested to be associated with peripheral insulin signaling and function of β-cells [82–84].

1.2.1. Atorvastatin

Atorvastatin is one of the synthetically produced statins. It is a lipophilic compound. The drug is commercialized by Pfizer Inc. at doses of 10, 20, and 40 mg as white, film-coated tablets. Atorvastatin is different from some of the statins since it is an active hydroxy acid, opposite to the inactive lactone prodrugs lovastatin and simvastatin. The statins that were developed later on chronologically, including atorvastatin, have open rings in their chemical structure which do not need re-opening in the liver or the gastrointestinal tract, unlike closed ring lactone structures in lovastatin and simvastatin [74,79,85].

From the pharmacological aspect, atorvastatin shares the main mechanism with other statins, prevention of the conversion of HMG-CoA in the liver. However, it was reported that these agents do not inhibit cholesterol synthesis completely and necessary cholesterol levels remained for vital functions such as sterol synthesis. Studies reported that atorvastatin does not affect the levels of cortisol in plasma and adrenal glands [79].

Atorvastatin is absorbed after oral administration quickly and reaches maximum plasma concentration within 1-2 hours. The duration of absorption is dependent on the given dosage and the maximum half-life is approximately 23 hours. Atorvastatin enters cells by membrane interaction directly and it is metabolized by cytochrome P450 3A4 (CYP3A4) which is a common pathway for other statins, lovastatin, and simvastatin [79,85].

The antilipidemic effect of atorvastatin is well studied in primary hypercholesterolemia and dyslipidemia patients. Reductions in LDL cholesterol (LDL-C) and total cholesterol were achieved within the 2-4 weeks of treatment. In the study of Brown et al. 32% of patients with CVD achieved LDL-C goal (>130 mg/dl) with 10 mg atorvastatin treatment for 12 weeks and this number increased to 83% with increased dosage of the treatment up to 80 mg [86]. In a large-scale randomized study, Atorvastatin Comparative Cholesterol Efficacy and Safety Study (ACCESS), atorvastatin, simvastatin, pravastatin, lovastatin, or fluvastatin treatment was applied with minimum recommended doses of 3916 patients with hypercholesterolemia [87]. Among the atorvastatin-treated group, 76% of patients achieved the LDL-C goal which is a significantly larger population than all of the other statin groups [88].

Intima-media thickness (IMT) of the arteries is an available marker to evaluate the progression of atherosclerosis. In the study to compare atorvastatin and simvastatin, it was reported that 80 mg atorvastatin treatment for 2 years resulted in a 51% reduction in LDL-C and in addition significant decrease in IMT of carotid arteries. On the other hand, a 41% reduction in LDL-C and only inhibition of IMT progression were observed in the simvastatin group [89]. In another large-scale randomized trial with atorvastatin or pitavastatin-treated 161 CVD patients, it has been reported that the pitavastatin group had stabilized carotid IMT, however, the atorvastatin treated group showed a reduction in IMT which proves atherosclerosis regression [87].

1.2.2. Pleiotropic Effects of Atorvastatin

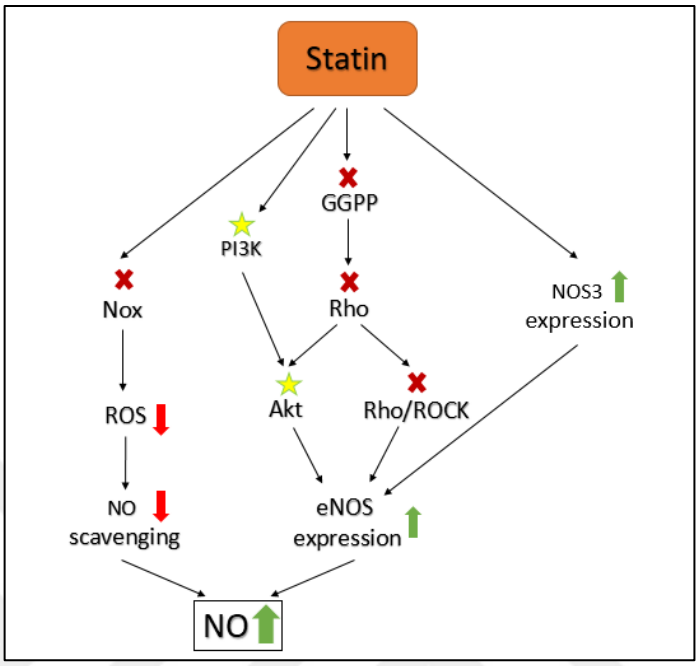

Figure 1.5. Pleiotropic effects of statin on pathways (modified from Garabi et al.) [90]

As previously indicated above, statins reduce the synthesis of cholesterol by inhibiting the HMG-CoA reductase enzyme. After this inhibition, an elevation of LDL-R and reduction in LDL deposition in the vascular walls are observed. Pleiotropic effects of statins are an important part of the treatment and advantage of statins as lipid-lowering compounds [90].

Suppression of apoptosis, regulation of immune response, anti-inflammatory effects, and neuroprotection are putative therapeutic effects ascribed to statins. eNOS is one of the important mediators of these effects. It has been reported in the literature that statins upregulate eNOS expression and NO bioavailability through different pathways (Figure 1.5). In the study of Mehta et al. expression of eNOS elevated by ox-LDL treatment in human coronary artery endothelial cells and 10 μM atorvastatin treatment decreased this elevation [91]. In another study with mice, 14 days of treatment with atorvastatin resulted in a 2.3-fold increased expression and 3-fold increased activity of eNOS.

Statins inhibit isoprenylation and post-translational modification of Rho protein because inhibition of HMG CoA reductase decreases the production of isoprenoid intermediates such as geranylgeranyl pyrophosphate (GGPP) [90]. This process causes the translocation of Rho

from the cytosol to the membrane and inactivates the protein. Inactivation of Rho by statins causes increased expression of Rho GTPase and inhibition of the Rho/Rho-kinase (ROCK) pathway. This mechanism results in the elevation of the half-life eNOS mRNA and the production of NO [92,93].

As indicated in the eNOS section (1.1.5.1) Akt activation is one of the important pathways in eNOS activation and NO production. Several studies reported that Rho inactivation by statin treatment increases Akt activation and subsequently eNOS activity is increased. Statins may also increase the transcription of NOS3 gene expression by microRNA regulation [92,94].

Increased ROS in the atherosclerotic area is an important mechanism in the plaque progression as explained above (1.1.6). One of the important pleiotropic effects of statins is decreasing ROS production [95,96]. This effect is important both for decreasing oxidative stress and also for increasing NO bioavailability since ROS may be bound to NO and can transform it into peroxynitrite. The inhibition of the Nox signaling pathway by statins is one of the actions of mechanisms for this effect [97]. In the study of Wassmann et al., it has been reported that atorvastatin treatment caused a decrease in the expression of Nox subunits, which is an oxidative-stress-producing enzyme [98]. Reduction of Nox results in decreased ROS and subsequently increased NO bioavailability by inhibiting NO scavenging. In addition, Nox inhibition increases NADPH levels which is a fundamental cofactor in NO synthesis by eNOS [20,90].

In conclusion, statins such as atorvastatin can influence several signaling pathways and molecules which subsequently increases NO production and availability in ECs.

1.3. TARGETED DRUG DELIVERY

In this fast-developing world of medicine, one of the most important problems is the delivery of drugs to their area of action in therapeutically effective dosage. Drug delivery systems are employed to achieve the ultimate goal to maintain disease-free conditions by solving obstacles related to physicochemical and molecular complexities caused by “free” drugs and under-dosing of the target [99,100].

Targeting the drugs involves adjusting the system to specific inclining to pharmacologically related targets in the body. Paul Ehrlich is the scientist who first mentioned about targeted drug delivery concept by referring to it as a “magical bullet” in the early 1900s [101]. In summary, targeted drug delivery involves the implementation of the drug to the patient, localization of this drug delivery system to the targeted pathological area, and release of the drug or therapeutic element in or around the area. In this way, nonspecific toxicity and adverse reactions are avoided, and administration of lower doses is achieved [99].

Targeted drug delivery could be achieved by invasive methods such as injection, catheter [102,103], gene-gun [104], etc. However, invasiveness is not preferable to the patient and most of these systems are highly expensive to carry out. Therefore, studies focused on noninvasive systems by either modification of drugs such as conjugating them with antibodies, peptides, aptamers, etc. to generate targeted prodrugs or drugs which can be loaded into nanocarriers. Nano-sized materials, which are accepted as <100 nm, are commonly used for the targeted delivery of drugs. Nano materials include micelles, liposomes, carbon tubes, and most commonly nanoparticles. All of these different types of nanomaterials have different features that allow them to carry specific drugs that have compatible chemical characteristics [100]. Nanocarriers provide several more advantages such as enhanced circulation time of drugs with or without modifying the surface of the nanomaterial. Coating nanoparticles with polyethylene glycol (PEG) is one of the most common modifications for increasing circulation time. Doxil®, Oncaspar®, and Genexol-PM® are examples of PEGylated nanoparticles that are currently used in clinics [105].

Targeting of the drug delivery system can be maintained either passively or actively. Passive targeting utilizes physicochemical and physiological factors for delivery. It works naturally in the body same as ligand-receptor binding for the hormones, neurotransmitters, growth factors, etc. [106]. Active transport on the other hand provides more control upon delivery of the drug. Modification and functionalization are applied to drug delivery systems such as attaching targeting moieties on the surface like antibodies, ligands, and aptamers to increase affinity towards specific markers on cells, tissues, or organs [107,108].

All of these benefits of targeted drug delivery have started new research for the treatment of CVDs to achieve either transform conventional therapeutics or develop new drugs. For example, in one study P-selectin targeting liposomes were loaded with vascular endothelial growth factor (VEGF) to provide better vascular structure and maintenance, and cytosolic

function in the post-myocardial infarction region [109]. In another study for the treatment of post-myocardial infarction, AT1 receptors targeted and conjugated liposomes with therapeutic payloads delivered to damaged heart cells. Results reported successful targeting, the better release of the drug, and increased accumulation in the targeted cells [110].

1.3.1. Targeted Drug Delivery in Atherosclerosis Treatment

Pathology of atherosclerosis provides an ironic advantage for developing targeted drug systems. ECs cover the inner layer of all vasculature, therefore it has a big potential for the introduction of nanomedicine. Abundant change of surface protein display on ECs and inflammatory changes in the atherosclerotic area provide a good opportunity for the application of targeted delivery [111]. Lewis *et al.* targeted CD36 scavenger receptors on the surface of macrophages which are abundantly found in atherosclerotic areas due to increased inflammation. Sugar-based amphiphilic macromolecules, which were designed to block C36 by competitive binding rather than ox-LDL, were compiled around the hydrophobic core and intravenously applied to mice. Results demonstrated that increased accumulation of NP on atherosclerotic regions and subsequently a decrease in lipid uptake, cholesterol levels, and occlusion of vessels was observed [112]. Liposomal nanoparticles are extensively used for the delivery of glucocorticoids to decrease inflammation in the plaque area. In the study of Lobatto *et al.* liposomal glucocorticoids were delivered to rabbits with atherosclerosis and they observed lower macrophage accumulation in the treatment group. Most importantly, these anti-inflammatory effects were obtained even in 2 days and this effect was displayed for up to 7 days at a minimum with a single dose [113]. This result demonstrates the advantages of targeted drug delivery in decreasing the given amount and increasing the efficacy of the drug.

As indicated in previous chapters, statins take the biggest portion in the treatment of atherosclerosis, however high dose of it has to be used to effectively maintain blood lipid at a normal range. In the study of Broz *et al.* pravastatin-loaded polymer vesicles functionalized with oligonucleotide sequences on the surface which allows them to target macrophages since there is a high yield of macrophages in that area. They successfully showed the internalization of the drug into macrophages and on the contrary, it had 15 times lower toxicity on muscle cells which indicates the capability of target-specific delivery of

pravastatin [114]. Nakashiro *et al.* used pitavastatin-loaded NPs for targeted delivery to circulating monocytes to inhibit plaque rupture of high-fat diet-fed ApoE (-/-) knockout mice. Results demonstrated that administration of the drug with NP reduced plaque destabilization by decreasing monocyte chemotaxis, on contrary any of these effects were observed by control NP or direct administration of the drug [115]. In another study of the same group, macrophages and monocytes in the ApoE (-/-) knockout mice were targeted for delivery of NPs that were loaded with pioglitazone, a peroxisome proliferator-activated receptor-γ agonist since it has the potential to inhibit plaque rupture by inhibiting proteinases secreted by macrophages. They showed NPs accumulated in aortic macrophages successfully and weekly administration of NPs for 4 weeks decreased plaque rupture marker in the brachiocephalic arteries which is a result that not obtained with control NP or an equivalent dose of drug [116]. Enhanced angiogenesis observed within atheroma can increase the severity of the disease. Therefore in one study, an anti-angiogenic component, fumagillin, was delivered to the neovascularization area by paramagnetic NPs targeting αvβ3 integrin which is a marker of neovascularization. As a result, significantly decreased angiogenesis was observed in addition to low side effects [117].

All of the studies explained above proved the potential of nanomedicine in the treatment of atherosclerosis. However, only a few nanomedicine techniques are clinically approved. Endothelium drug delivery has several challenges such as diverse size of arteries, shear stress by blood flow and margination, and red blood cells (RBCs) accumulation in the center of blood vessels. The main goal is achieving the effectively binding of NPs to micro, small, medium, and large vessels despite the continuous flow. Therefore, studies mostly focused on targeting adhesion molecules and selectins [118–120]. In the present study ICAM-1 selected as target to deliver atorvastatin. Apart from being an accessible binding component for nanoparticle, targeting ICAM-1 allows targeting inflammation and subsequently pre-atherosclerotic step since inflammation is the initial step of atherosclerotic plaque formation as explained above.

1.3.2. Aptamers

Aptamers are designed and apprehended as strong therapeutic and diagnostic biological tools, fundamentally because of their capability to be selected for a variety of disease and drug targets [121].

Aptamers are single-stranded (ss) DNA or RNA sequences with the capability of binding a target molecule with their unique tertiary structure. Systematic Evolution of Ligands by Exponential Enrichment (SELEX) is the screening method for aptamers. The aptamer is first used by Tuerk in 1990 as a term that is a combination of two words from Latin "Aptus" which means "fit" and "meros" which is translated as "particle" [122].

Aptamers are capable of interacting and binding to their targets including large protein complexes, simple inorganic molecules, and whole cells with high affinity and low dissociation constant by structural recognition which allows them to be referred to as "chemical antibodies"[123]. Antibodies have several disadvantages compared to aptamers. First of all, the production of antibodies takes several months while aptamer production takes a few hours. In addition, there is very low batch differentiation and immunogenicity in aptamers compared to antibodies. Also, aptamers are very stable, cost-effective, and can be stored for a long time [124].

Apart from their targeting capabilities aptamers are used as therapeutics. A good example is VEGF inhibiting aptamer, pegaptanib (i.e., Macugen®), for treatment of age-related macular degeneration which is FDA approved and currently used in clinics. Another example of a potential aptamer drug is AS1411 for the treatment of acute myeloid leukemia which is under clinical testing.

1.3.2.1. Systematic Evolution of Ligands by Exponential Enrichment (SELEX)

The selection of aptamers is held by in vitro protocols called SELEX which is a highly effective method for the elimination of high-affinity oligonucleotides, such as aptamers, from a wide range of random sequences. As the first definition of aptamers, the SELEX method is also firstly created in 1990 to isolate RNA sequences. From the begging till 2007, SELEX methods is used for RNA isolation since RNA was thought to be able to fold and form a spatial structure that allows it to bind target molecules. However, later studies indicated that ssDNA molecules are also capable of binding to the target molecule. After this

information DNA aptamers occupied a bigger part of SELEX studies. Nevertheless, it is known that both DNA and RNA aptamers have similar affinities for several small molecules. In the present study, an ssDNA aptamer that targets ICAM-1 was used. ICAM-1 targeting aptamers have been used in some studies including inhibition of migration and invasion of cancer cells [125] and detection of metastatic potential by measuring ICAM-1 protein in blood [126].

SELEX protocol consists of recurrent cycles of incubation, binding, partitioning, and amplification. The first step of SELEX is the design of a proper oligonucleotide pool which consists of 10^{14} to 10^{15} different sequences for a successful application. Those sequences have a random sequence with a flanked region with fixed sequences for both sides which are binding sites for primers. Target molecules are incubated in an oligonucleotide pool after incubation weakly bound sequences are washed away. At portioning, step sequences with high affinity are isolated and amplified by polymerase chain reaction (PCR) or reverse transcriptase PCR in the case of RNA aptamers. After 10-15 cycles aptamers which has a high affinity to the target are obtained (Figure 1.6).

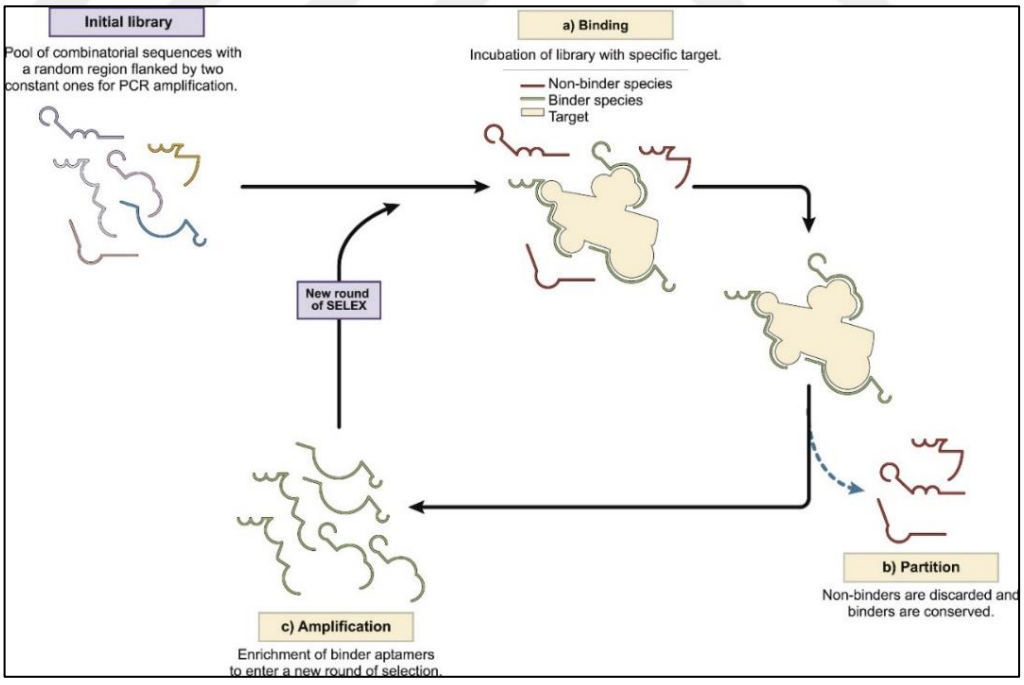

Figure 1.6. Aptamer selection by SELEX [127]

There are different SELEX methods with the same purpose but have additional different steps. Traditional SELEX as described above uses purified target molecules which is not the

case in vivo. Therefore, CELL-SELEX is the method that uses specific targets on cell membranes that might be preferred in some cases to consider the effect of other molecules in the environment. To select aptamers that are physiologically representative and bind to tumor tissue or any other organ in vivo, SELEX might be used. This method starts with the injection of the initial library to an animal after that unbound aptamers will be discarded through the kidney and bind aptamers are elucidated directly from the tissue by DNA/RNA extraction and followed by PCR step. After several steps of this cycle, a high-affinity aptamer to the desired tissue is obtained [124,127]. In the colorectal cancer study of Mi et al. after 14 cycles, they obtained an aptamer that binds and blocks the activity of oncogenic helicase p68 which is upregulated in tumors [128].

1.3.2.2. Aptamer Gated Nanoparticles (APT-NP)

In this study ICAM-1 aptamer gated mesoporous silica nanoparticles (MSNs) were used as a targeted drug delivery system.

In the past two decades, one of the top focuses of aptamer studies was cardiovascular disorders since finding a cardiac biomarker-based drug delivery or diagnostic tool would help treatment of malfunctioning in the cardiac system and further could reduce the global mortality rate (33). Cardiac biomarker-based therapeutic tools for CVD have become a critical research priority throughout the last century. A couple of studies with aptamers focused on targeting the von Willebrand factor (vWF) which is known to be increased thrombosis and hemostasis. DNA aptamers referred to as ARG1779 and ARG1772 target subdomains of activated vWF on platelets [129]. This reaction creates a reversible anti-platelet effect. Another example of aptamer usage in CVD treatments is direct inhibition of thrombin by ARG183 binding [130]. In addition, REG1 aptamer functions in inhibition of thrombin by targeting factor IX which has a role in thrombin generation [131]. Even though these studies focus on several CVDs, targeted drug delivery research focusing on CVDs and especially atherosclerosis treatment by aptamers is still limited [132].

Several nanoparticle formulations are currently used in research and clinics. However, silica nanoparticles have become the focus of nanomedicine research over recent years. In the present study, Mobile crystalline material number 41 (MCM-41 type), a variant of MSNs, is used as drug carriers which are silica nanoparticles with mesopores. MSNs consist of an amorphous silicon dioxide (silica) matrix and according to IUPAC, they must have a pore size between 2-50 nm. MSNs have several advantages including forming uniform pores with

adjustable size, high surface area and a high pore volume, easy functionalization of the surface, and compatibility with the gating mechanism of pore opening internally and externally [133]. All these modifiable features of MSNs allow them to be tailored for carrying a very diverse range of drugs, both hydrophobic and hydrophilic which makes MSNs a promising drug carrier. Several studies reported successful results of carrying drugs, proteins, DNA, and RNA molecules [134]. In addition, they are developed for enhancing the treatment of several diseases including breast cancer [135], colorectal cancer [136], allergic inflammation [137], and osteoporosis [138] among others.

The novelty of the targeted drug delivery system used in the present research includes the controlled release of the drug in the targeted area which has been explained in previous studies [139–141]. Aptamer moiety of the APT-ATS-NP acts as a gate for the controlled release of atorvastatin. This is achieved by bonding aptamers to silica nanoparticles by covalent bonds. As a result of this covalent bonding, aptamers do not detach from the nanoparticle even though there is a high affinity towards the target, which is in contrast with most of the delivery systems with aptamers [141].

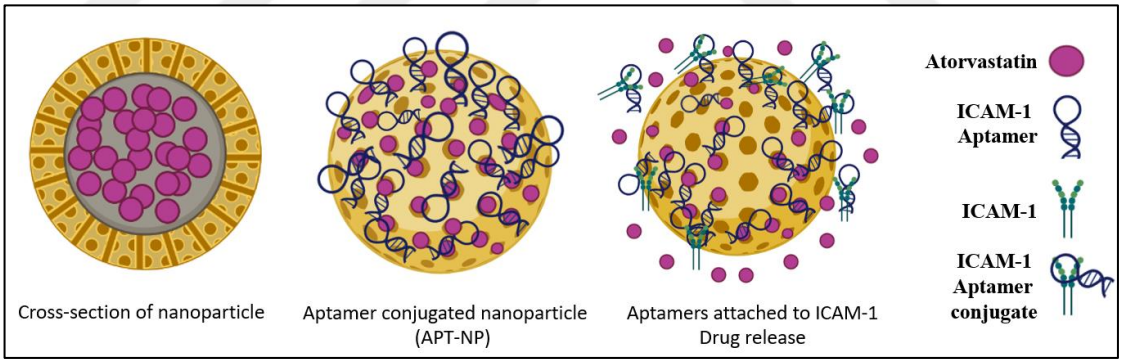

Figure 1.7. Representative illustration of nanoparticles

Achieving regression and stabilization of atherosclerotic plaques at late stages of the disease is hard therefore delivery of atorvastatin to the atherosclerotic area at early stages is critical for effective treatment. Therefore, in the present study ICAM-1, an inflammatory biomarker, targeting aptamer gated nanoparticles delivered atorvastatin to HUVECs during exposure to low shear stress to mimic pre-atherosclerotic conditions. In order to assess the effects of APT-ATS-NP intracellular ROS levels, eNOS and Akt protein expression and phosphorylation levels were measured.

2. MATERIALS

2.1. INSTRUMENTS

Table 2.1. Instruments

Material	**Brand**	**Catalog No**
Power Supply	Cleaver Scientific	POWERPRO300
Tube heater	Bioer Technology	CHB-A4-HH
Orbital Shaker	Alfagen	OS-100
ChemiDox XRS+	Biorad	1708265
Flow Cytometry	Beckman Coulter	Cytoflex S
Electrophoresis System	Thermo Fischer	EI0001
Trans-Blot Electrophoretic Transfer Cell	BioRad	1703930

2.2. CONSUMABLES

Table 2.2. Consumables

Material	**Brand**	**Catalog No**
Cell Culture Flask	SPL	70025/70075
Cell Culture Flask	Corning	430641U
Bis-Tris precast Gels	Abcam	ab270467
Ibidi slide (1u-Slide 1^0,4 Luer ibiTreat)	ibidi	171211/4
Serological Pipette 5ml, 10ml, 25ml	Costar	4487/ 4488/
Centrifuge Tubes 5 ml, 15ml, 50ml	Falcon	352070
Microentrifuge Tubes 1.5 ml	Capp	5100500
Micropipette Tips 10µl, 200µl, 1000µl	Capp	5030010/5130070/ 5130130
24 well plates	Costar	3526
Western Blotting Filter Paper	Thermo	88600

2.3. CHEMICALS

Table 2.3. Chemicals

Material	**Brand**	**Catalog No**
20X Running Buffer	Novex	B0002

Akt mAb	Cell Signalling	9272S
Atorvastatin	Sigma	PZ0001
DC Protein Assay Reagent A	Biorad	500-0113
DC Protein Assay Reagent B	Biorad	500-0114
DC Protein Assay Reagent S	Biorad	500-0115
DCFDA / H2DCFDA - Cellular ROS Assay	abcam	ab113851
Dimethyl Sulfoxide (DMSO) %99,9	Sigma	D8418
DMEM	Gibco	41965-039
DPBS	Gibco	14190-094
ECL	Thermo Fischer	1859023/1859022
eNOS mAb	Cell Signalling	9586S
FBS	Gibco	10500-064
Fibronectin, Human	Corning	354008
Fluorescein Phalloidin	Molecular Probes	F432
GAPDH mAb	Boster	M00227
Glycine	Invitrogen	1836C513
MES SDS Running Buffer	Invitrogen	B0002
Methanol	Umaylab	67-56-1
NaCl	Isolab	7647-14-5
pAkt mAb	Cell Signalling	9671S
Penicillin/Streptomycin	Gibco	15140-122
peNOS mAb	Cell Signalling	9571S
Protease & Phosphatase Inhibitor	Thermo Fischer	78444
Protein Ladder	BioLegend	77302
Resolving Buffer	Invitrogen	HC2212
RIPA	Thermo Fischer	89900
Secondary Antibody Anti-Mouse	Abcam	ab6789
Secondary Antibody Anti-Rabbit	Abcam	ab6789
Sheath Fluid	Beckman Scientific	B515003
Skim Milk Powder	Oxoid	LP0031
Stacking Buffer	Invitrogen	HC2112
Stripping Buffer	Thermo Fischer	46430
TG2 mAb	abcam	ab2386
Tris	Thermo Fischer	17926
Tris HCl	Sigma	T5941-500G
Trypsin	Gibco	25200
Tween-20	Neolab	1247ML500

3. METHODS

3.1. STUDY DESIGN

In this study, the effects of targeted delivery of atorvastatin via ICAM-1 aptamer gated silica nanoparticles were examined on HUVECs under static and atherosclerosis mimicking shear stress conditions (Figure 3.1). To investigate the effect of atorvastatin concentrations eNOS, peNOS, Akt and pAkt protein levels were measured by Western Blotting and intracellular ROS was measured by flow cytometry.

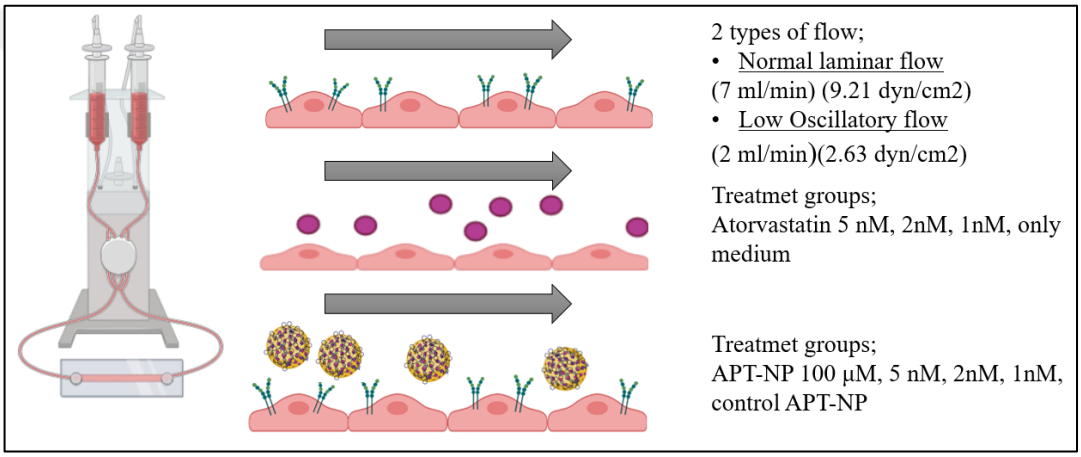

Figure 3.1. Graphical abstract of cell culture design

3.2. SYNTHESIS OF NANOPARTICLES

ICAM-1 aptamer gate

(ACACCATAGTAGCAATGGGCACCACTAGTACACAGTAGCACACCAGTAGTC) was synthesized by Sentromer Ltd (Istanbul, Turkey). Converting of an aptamer sequence to the gate was described for Staphylococcus aureus aptamers as well as small molecules like ATP [142,143].

50 mg of MCM-41 powder (Sigma-Aldrich, 643645) with 1 ml (95% ethanol containing 5% 1 mM of acetic acid) was stirred for 1 hour at room temperature. 500 µl (3-Aminopropyl) triethoxysilane (Sigma-Aldrich, APTES) (440140) was added and followed by overnight

incubation under mixing. (MCM41/APTES ratio=5). Then, nanoparticles (NP) were washed 3 times and dissolved with PBS.

For drug loading, silica NP was incubated in atorvastatin in PBS overnight as described for other small molecules with similar molecular weight to atorvastatin.

Aptamer gated atorvastatin-loaded silica NP (APT-ATS-NP) were characterized using Transmission Electron Microscopy (TEM), Dynamic Light Scattering (DLS), Fourier Transform Infrared Spectroscopy-Attenuated Total Reflectance (FTIR-ATR).

3.3. APTAMER GATED NANOPARTICLE CHARACTERIZATION AND MEASUREMENTS

Characterization of ICAM-1 aptamer gated silica nanoparticles made by TEM imaging.

3.3.1. TEM Analysis

TEM analyses were performed to obtain morphological, compositional, and crystallographic information about samples. The first step of preparation of MCM-41 particles is ultrasonication of powders in ethanol for 15 min. Secondly, particles are applied onto a copper carbon-coated grid by drop-casting method to dry a droplet of suspension. TEM analysis was carried out on JEM 2100 Plus Electron Microscope – JEOL in Yeditepe University.

3.3.2. DLS Analysis

To analyze the average hydrodynamic size distribution of APT-ATS-NP, the DLS technique was used. It was performed with Zetasizer Nano-ZS, (Malvern Instruments, Worcestershire, UK) (Yeditepe University).

3.3.3. FTIR Analysis

Characterization of amide bond formation on the surfaces of SiO_2 nanoparticles was performed with FTIR-ATR analysis. A spectrum scan of wavelengths between 200-900 nm, 1 ml of nanoparticle samples in PBS before and after APTES functionalization by IS50 FTIR Nicolet Thermo Ficher with ATR.

3.4. CELL CULTURE

HUVECs were purchased from ATCC (CRL-2873) and cultured in Dulbecco's Minimum Essential Medium (DMEM) with %10 Fetal Bovine Serum and %1 Penicillin/Streptomycin. Passage 11-15 are used during whole experiments. Previously frozen cells were thawed at a 37°C water bath. Thawed cells were transferred into 15 ml tubes and ~10 ml DMEM was added on top of it to dilute the DMSO amount that was used in the freezing process. Further on, the cell suspension was centrifuged at 500 RCF for 5 minutes and the pellet dissolved in fresh ~1 ml DMEM. Cells were transferred to either T25 or T75 flasks and a proper amount of DMEM was added to fill the flask. Throughout the study, cells were incubated at 37°C %5 CO_2 incubators. ~%80 confluent cells are used for further experiments or confluent flasks passaged and the medium of the cells is changed every 2-3 days. To passage cells old medium was removed and cells were washed 2 times with 3-7 ml Dulbecco's Phosphate Buffer Saline (DPBS) to discard any leftover Ca+2 or Mg+2 which might inhibit the enzymatic activity of trypsin. After the washing step for the T25 flask 0.5 ml, for the T75 flask 1ml trypsin was added on top of the cells gently and then an equal amount of DPBS was added to trypsin to cover the surface area and to dilute the trypsin. Flasks were incubated at 37°C for approximately 5 minutes. Cells were re-suspended and trypsin activity was inhibited by the addition of DMEM. 10 ul cell suspension was taken onto the hemocytometer to count cells and an appropriate amount of cells were transferred into a new tube. Cells were centrifuged at 500 RCF for 5 min and seeded on a new flask after resuspension with DMEM. The rest of the cells were frozen and stored at -80°C in %5 DMSO containing DMEM.

3.4.1. Atorvastatin and APT-ATS-NP Concentration Calculation

Atorvastatin (Sigma, PZ0001) stock is prepared in DMSO. The molecular weight of atorvastatin is 604.69 g/mol. 18 mg Atorvastatin weighted and dissolved in 495 µl DMSO to obtain 60 Mm stock. The final concentration of DMSO in the DMEM was less than 0.1% and did not affect cell viability.

The first batch of APT-ATS-NP had 0.28 mg Atorvastatin in 1 mg NP. ~0.13 mg APT-ATS-NP weighted and dissolved in 12ml DMEM to obtain the final 5 nM atorvastatin concentration in flow conditions. ~0.05 mg weighted APT-ATS-NP weighted and dissolved in 12 ml DMEM for 2 nM final atorvastatin conditions and same weight dissolved in 24 ml DMEM for 1 nM final atorvastatin concentration.

The second batch of APT-ATS-NP 0.42 mg atorvastatin in 1 mg NP. ~2mg APT-ATS-NP weighted and dissolved in 15ml DMEM for final 0.1 mM Atorvastatin concentration.

3.4.2. Static Conditions on HUVECs

To investigate the effect of different atorvastatin concentrations (40 µM, 10 µM, 5 µM, 1 µM, 5nM, 2nM, 1nM) on HUVECs under static conditions cells were seeded on 24 well plates. ~200k cells were seeded to each well and left overnight in an incubator. The next day all medium was removed and DMEM that contains different atorvastatin concentrations and only DMEM as control were added to wells in triplicates and left for incubation for 24 hours. After incubation cells were lysed and proteins were isolated.

3.4.3. Shear Stress Exposure to HUVECs (Flow Conditions)

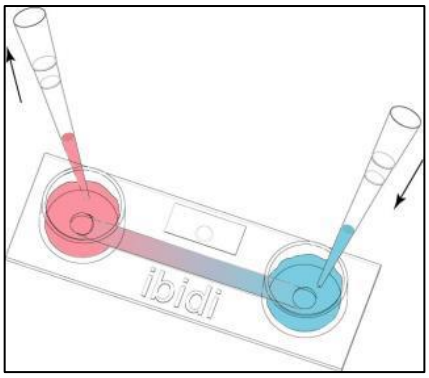

Figure 3.2. Ibidi µ-Slide (from Manufacturer's Manual)

HUVECs were seeded into IBIDI slides (1 µ-Slide $1^{0.4}$ Luer iBiTreat) (Figure 3.2) in a portion of 120.000 cells per slide to reach confluency. Before cell seeding slides were coated with fibronectin as recommended in the manual at a concentration of 75 µg/ml. Fibronectin solution was prepared by dissolving 0.3 mg fibronectin in 4 ml DPBS and stored at +4°C for up to 3 weeks. Prior to cell seeding slides are filled with 100 µl fibronectin solution and incubated for 20-30 min at room temperature. Excess fibronectin was washed away by 1ml DPBS. After that HUVECs are seeded in a concentration of 120.000 cells in 100 µl DMEM and slides incubated in %5 CO_2 37°C overnight for cell attachment.

On the same day, reservoirs of the IBIDI Fluidic Unit were filled and left for overnight equilibrium in an incubator with DMEM regarding the experimental group. For atorvastatin only groups ~12ml DMEM containing 5nM, 2nM, or 1nM of atorvastatin prepared from 60 mM atorvastatin stock that dissolved in DMSO previously. Nanoparticles start to release the drug when they are dissolved in liquid, even though the release amount is not high we still did not leave the nanoparticle-containing DMEM for overnight equilibrium. Instead 10ml DMEM for 5nM and 2nM group, 20 ml loaded for 1nM to fluidic unit for overnight equilibrium. The next day nanoparticles were weighted as needed; for 5nM ~125 µg dissolved in 2ml DMEM, 2nM 50 µg dissolved in 2ml DMEM and for 1nM 50 µg in dissolved in 2ml DMEM, and nanoparticle-containing DMEM was added to the fluidic unit inside the incubator. As a control group, the same LOF conditions were applied to HUVECs with DMEM that do not contain any treatment.

The medium of the slides that were incubated overnight was changed by syringe and pipet. Reservoirs were filled to the top to form a bump to prevent air bubble formation during connection to fluidic units. 3 slides were connected and the free reservoirs are connected to the fluidic unit for a continuous uniform flow through all 3 slides. (Figure 3.3 and 3.4)

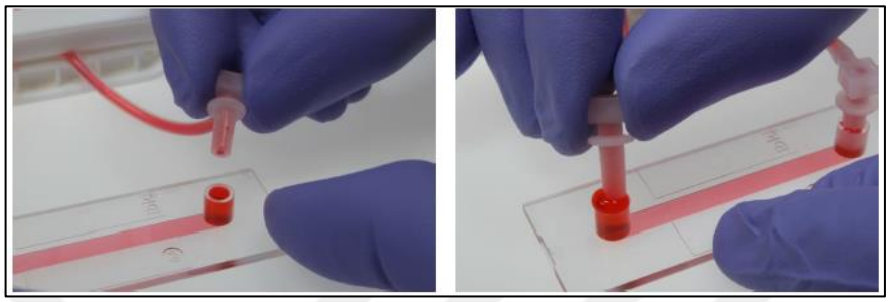

Figure 3.3. Connection of Ibidi µ-Slide's to the system (from Manufacturer's Manual)

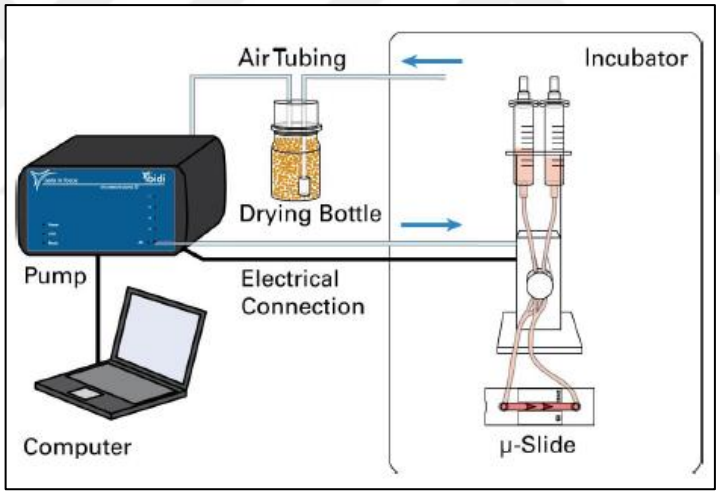

Figure 3.4 Representative image of complete Ibidi system (from Manufacturer's Manual)

3.4.3.1. Digital Control Setup of Shear Stress

PumpControl Software was installed on the computer to which the IBIDI air pump was connected to set up the flow rate and flow type. First of all perfusion set and slide type was chosen from Fluidic Unit Setup tab from PumpControl Software. We used red perfusion set with an inner diameter of 1.6 mm throughout the experiment. For normal flow samples, a 7 ml/min flow rate is set, and the software automatically calculates shear stress as 9.21 dyn/cm^2. For oscillatory flow, two fluidic units are needed. Fluidic units were connected to the air pump as described in the manual. The flow rate is set at 2 ml/min and shear stress

was calculated as 2.63 dyn/cm^2. For the fluidic unit that the slides were connected to, the oscillating flow was chosen from the Flow Parameters tab on PumpControl Software.

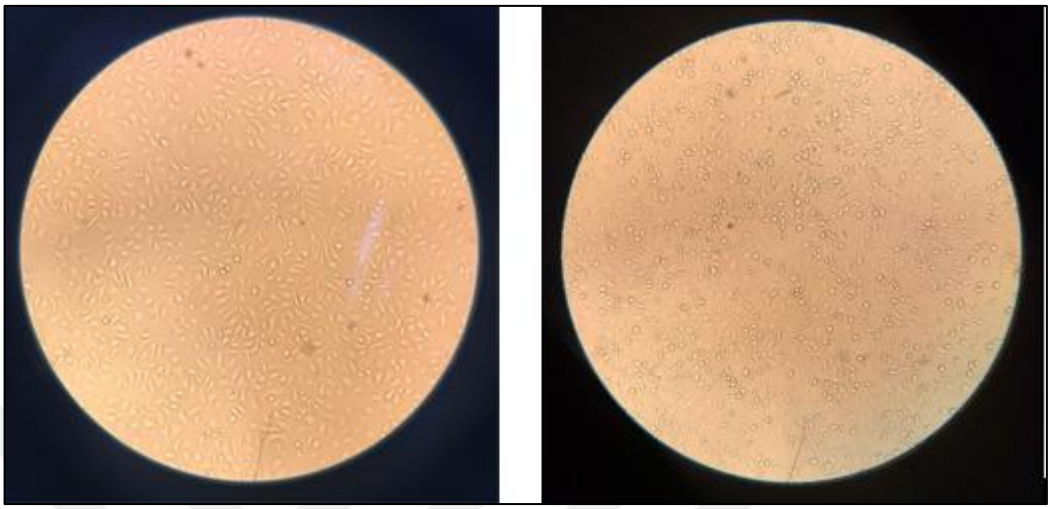

Figure 3.5. Representative microscope images of HUVECs. The left image indicates before and right image indicates after flow conditions.

3.5. INTRACELLULAR ROS MEASUREMENT BY FLOW CYTOMETRY

Measurement of intracellular ROS was performed by DCFDA staining. The same procedure for cell seeding and flow application was applied with 2 connected slides. For unstained control and static control, cells were seeded with the same procedure however they were not connected to the flow system 10 µM DCFDA solution was prepared by adding 1 µl DCFDA (20mM stock) to 1,999 ml phenol red-free DMEM. At the end of the 24-hour flow application, the Ibidi flow system was stopped and the medium inside the slides was changed by the previously prepared 10 µM DCFDA solution except for the unstained control slide, which was changed with a phenol red-free medium. Cells were incubated with DCFDA solution for 30 minutes. After incubation DCFDA solution was washed away from slides by DPBS gently. 100 µl trypsin was added to slides and incubated for 5 min in the incubator. Detached cells were collected in phenol red-free medium and cells were centrifuged at 300 RPM for 3 minutes and 500 RPM for 1 minute to discard trypsin. After discarding of supernatant, the pellet was dissolved in a 200 µl phenol red-free medium and transferred immediately to a 96 well plate for flow cytometry. All experiments with DCFDA were held in dark conditions since it is a light-sensitive chemical.

Flow cytometry measurement was performed by Beckman Coulter Cytoflex S device and CytExpert Software. 10^5 event was read for each sample. Experiments were repeated three times. Mean FITC values were used and results were represented relative to static control.

3.6. MEASUREMENT OF PROTEIN EXPRESSION LEVELS BY WESTERN BLOT

3.6.1. Protein Isolation

Protein isolation from the 24-well plate was started by removing the old medium and washing each well with 1 ml DPBS. For lysing the cells, after removal of DPBS from the first well of each group, 200 ul lysis buffer that contains RIPA with protease/phosphatase inhibitor (1x) and EDTA (1x) was added to empty wells and incubated 5-7 minutes at room temperature. DPBS from the 2nd well of each group was removed and lysis buffer was transferred from 1st well to 2nd and all processes were repeated for the 3rd well. The lysate was collected from the 3rd well and centrifuged at 14000 g for 10 minutes at +4°C. The supernatant was transferred to a new microcentrifuge tube and stored at -20°C until western blotting.

Protein isolation from IBIDI slides was performed according to the manual. The first medium inside the slide was removed. Slides were washed with 1 ml cold DPBS and filled with DPBS again. Lysis buffer contained RIPA with protease/phosphatase inhibitor (1x) and EDTA (1x). DPBS from one of three slides was removed and 100 µl lysis buffer was added inside the slide with a pipette and left for incubation on ice for 7-10 minutes. To make sure that all cells were removed pipetting was applied with a syringe. DPBS was removed from another slide and lysate from 1st slide was transferred to an empty slide and all processes were repeated for the last slide. Finally, the lysate was transferred into a new microcentrifuge tube and centrifuged at 14000g for 10 minutes at +4°C. Supernatant stored at -20°C until western blotting.

3.6.2. Detergent Compatible Protein Assay

To quantify the total protein amount DC assay was performed according to the manufacturer's protocol. 1.5, 1, 0.5, 0.25, 0.125, 0.05 mg/ml BSA concentrations used as standards. 5 µl from each sample and each standard was added to 96 well plates in duplicates. 25 µl of reagent A that contains reagent S was added on top of wells. Afterward, 200 µl reagent B was added to each well while lights were turned off. Plate incubated for 15 minutes in dark. After incubation absorbance was measured at 750 nm by a plate reader. Standard curve and concentration calculations made with Excel. The same number of cells was used for each group in both static and flow conditions. Therefore, small differences in the total protein concentration were neglected, and the same volume of samples was used in western blot.

3.6.3. SDS-PAGE

Protein separation was performed with %4-12 Bis-Tris precast gels. 19.25 µl protein isolate of slide samples from each group was transferred into a 0.5 µl tube. 19.25 µl sample contained ~20 µg total protein according to DC assay. Because of the optimization process for static condition samples total protein amount that was loaded varies between 10ug to 40ug. However, the amount was the same in each gel and all the results were normalized to GAPDH bands. To obtain better results maximum volume from samples was taken, according to the manual maximum volume for wells on the gel is 35 µl. 8.75 µl sample buffer and 3.5 µl reducing agent were added to the tube in order. Tubes were incubated on the heater at 95°C for 10 minutes, followed by 10 minutes on ice. Each sample and 4 ul protein ladder were loaded to gel. 1x MES Running Buffer previously diluted from 20x stock with dH2O, was poured into the running tank as filling the inner chamber until the surface and outer chamber the ¾ of the tank. Running started at 120 V for 15 minutes, followed by 1 hour 130 V and ~1 hour 140 V. Running was stopped when the 15kDa protein ladder line was close to the bottom.

3.6.4. Western Blotting

Relative protein expression was measured by western blot. The gel was transferred to the PVDF membrane by wet transfer with 85 V for 15 hours. Transfer buffer (10x) prepared by addition of 144 gr Glycine and 30.2 gr Tris-Base to 1 L deionized water and solution was mixed until it becomes clear. pH measured as ~8.3. To obtain 1x transfer buffer solution 100 ml 10x solution, and 100 µl %96 Methanol was added to 800 µl dH2O. Tris Buffer Saline (TBS) was prepared as a 10x stock solution and 1x buffer was used throughout all experiments. TBS was prepared by dissolving 26 gr Tris-HCl, 5.6 gr Tris Base, and 88 gr NaCl in 1 l dH2O. pH measured approximately 7.6. TBS-Tween20 (TBS-T) contained 1x TBS solution and %0.1 Tween-20.

After the transfer was completed, the membrane was washed with TBS-T for 2-3 minutes. The membrane was incubated with %5 skim milk powder in TBS-T at room temperature on an orbital shaker (90 rpm) for 1 hour. The membrane was cut by regarding necessary protein ladder line. Each membrane was incubated with proper primary antibody overnight (~18hour) in the cold room (+4°C) on an orbital shaker (90 rpm). Membranes were washed 3 times 5-7 minutes with TBS-T after overnight incubation on an orbital shaker (120 rpm). Secondary antibodies were applied to membranes and incubated for 1 hour at room temperature on an orbital shaker (90 rpm) (Table 3.1.). Lastly, membranes were washed 3 times 7-10 minutes with TBS-T on an orbital shaker (1200 rpm) and stored in TBS-T +4°C until imaging.

Table 3.1. Antibody dilutions for western blotting

Antibody Name	Primary Antibody Dilution	Secondary Antibody Dilution
eNOS	1/300	1/5000
peNOS	1/300	1/5000
Akt	1/2000	1/10000
pAkt	1/2000	1/10000
TG2	1/5000	1/25000
IL-6	1/5000	1/7500
GAPDH	1/5000	1/50000

3.6.5. Imaging and Analysis

Imaging was done with the ChemiDoc XRS+ device. Chemi High-Resolution option was used for all bands throughout all imaging. Exposure was limited by observing a saturated point at one of the bands. The image taken before that point was taken for analysis. The light of the machine was not working properly, therefore imaging of the ladder was not able to be done with the Marker option. UV Trans Illuminator was used instead of it. Analysis of the images was done with ImageLab 6.0.1. After the detection of lanes and bands, the area was limited by lane profile graphics. The background was subtracted at maximum for all analyses. All proteins normalized to GAPDH by dividing and relative band intensity calculated according to LOF conditions.

4. RESULTS

4.1. CHARACTERIZATION OF APT-ATS-NP

TEM images revealed the surface topography and morphology of the nanoparticles which are spherical. Also, TEM images exhibited the porous structure of the nanoparticles (Figure 4.1.). The hydrodynamic size of the silica nanoparticles is 284.8±17 nm (Figure 4.2.). Before and after amine functionalization, amine bonds were characterized (Figure 4.3.).

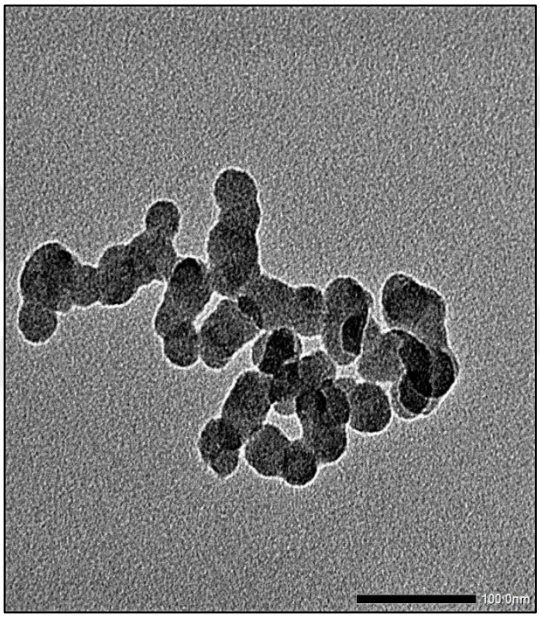

Figure 4.1. Representative TEM image depicting the morphology of MCM-41 type mesoporous silica NP

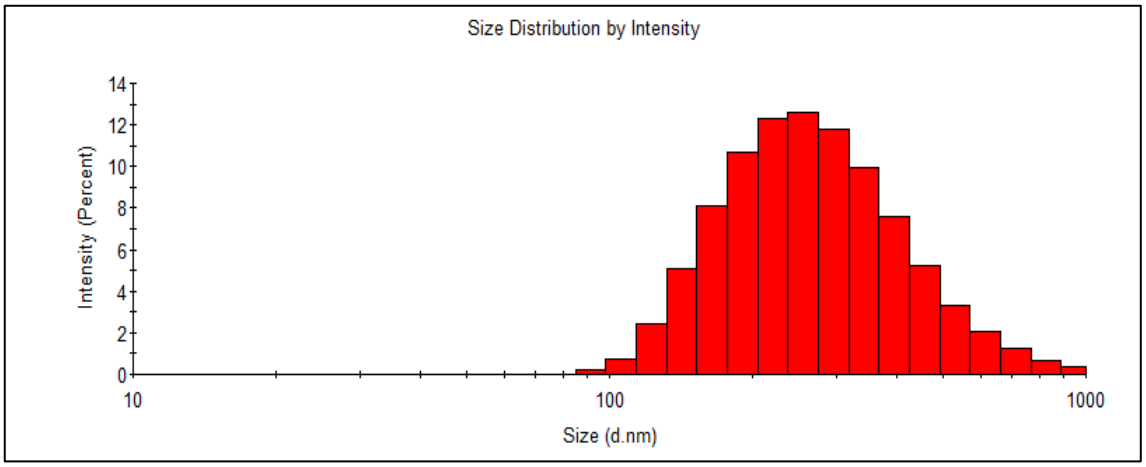

Figure 4.2. The average diameter of MCM-41 type silica NP used in the current study by DLS

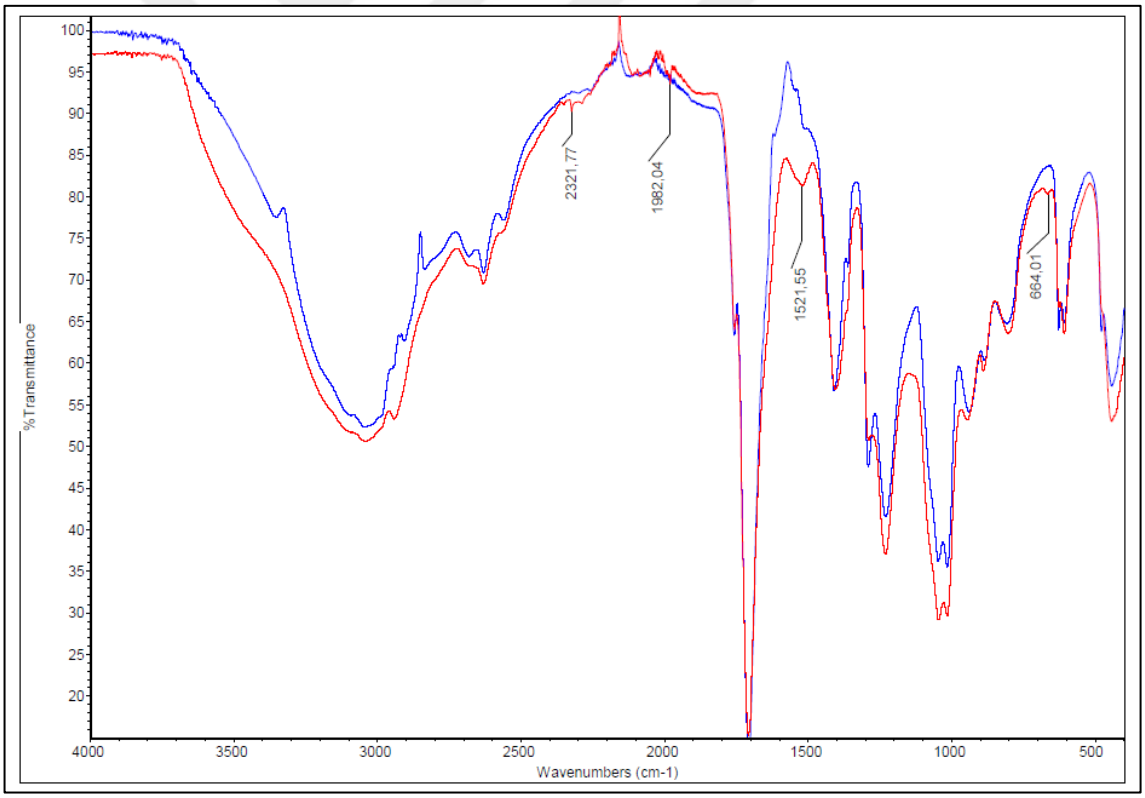

Figure 4.3. FTIR spectra of MCM-41 type silica NP after amino grafting (Red line represents silica NP with amine bond formation).

4.2. EFFECT OF FLOW CONDITIONS ON ICAM1 MRNA EXPRESSION

To validate the effect of LOF on ICAM1 mRNA expression qRT-PCR was performed in previous experiments [126]. Data obtained from these experiments revealed that LOF had an increasing effect on ICAM1 mRNA expression (~2.6 fold) in HUVECs when it is compared to NF. In addition, cells were exposed to unidirectional low flow (LF) (without oscillating). LF caused an increase in ICAM1 expression compared to NF. However, LOF had ~1.7 fold higher ICAM1 mRNA expression compared to LF (Figure 4.4). In conclusion, this data confirms that LOF is a better flow condition to mimic atherosclerosis in the context of increased ICAM1 mRNA expression. Therefore, it is a suitable target for atorvastatin delivery for the treatment of atherosclerosis.

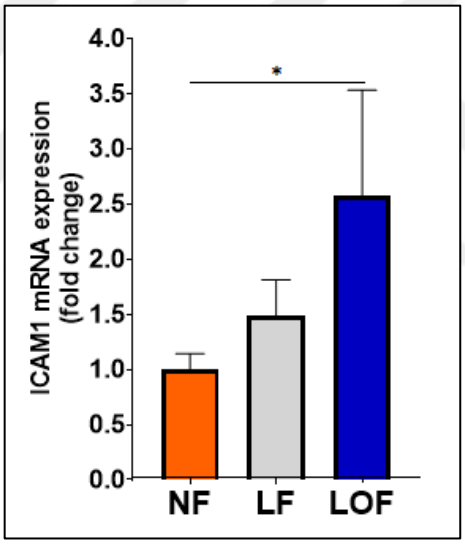

Figure 4.4. Effect of flow conditions on ICAM-1 mRNA expression. (NF: normal flow, LF: low flow, LOF: low oscillating flow) For statistical analysis, Student's t-test was performed. (* $p<0.05$, n=8, 7, 3 for NF, LF, and LOF groups, respectively.

4.3. EFFECT OF APT-ATS-NP ON INTRACELLULAR ROS LEVEL

To demonstrate the effect of atorvastatin delivery by APT-ATS-NP to HUVECs under LOF conditions, intracellular ROS levels were measured quantitatively by flow cytometry. The cells were treated with 0.1 mM atorvastatin or 0.1 mM atorvastatin releasing APT-ATS-NP as the final concentration. Treatment with ATS-APT-NP significantly reduced intracellular

ROS levels compared to atorvastatin treatment alone ($p<0.01$) (Figure 4.5 A, B). In addition, ROS levels in ATS-APT-NP treated group was significantly lower compared to the LOF group ($p < 0.05$) (Figure 4.5 A, B), however, this significant reduction was not measured with atorvastatin treatment alone. To demonstrate the effect of native NP (ctrl NP) on intracellular ROS levels under LOF conditions, cells were treated with silica NP which was not surface-functionalized and not loaded. Ctrl NP did not affect intracellular ROS levels compared to LOF. Moreover, APT-ATS-NP treatment significantly reduced intracellular ROS levels compared to Ctrl NP (Figure 4.5B).

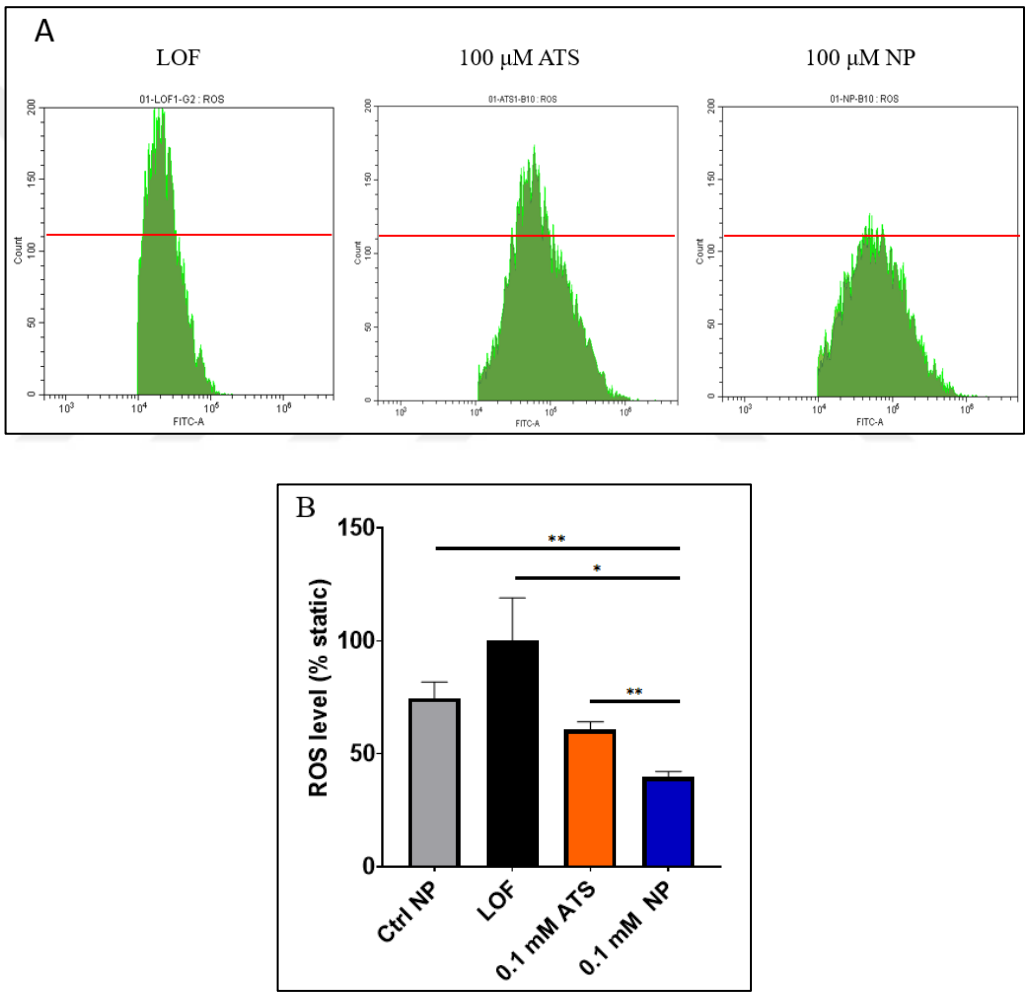

Figure 4.5. Intracellular ROS levels of HUVECs treated with APT-ATS-NP under LOF conditions. A) Representative histograms of intracellular ROS levels measured by flow cytometry. B) Mean intracellular ROS levels normalized to static control. (ctrl NP: native NP, LOF: low oscillating flow) For statistical analysis, Student's t-test was performed. (* $p<0.05$, ** <0.01, n=16, 8, 6, 6, 5 for static, LOF, ATS, NP and CTRL-NP groups, respectively.

4.4. EFFECT OF ATORVASTATIN ON ENOS AND AKT PROTEIN EXPRESSION LEVELS

To investigate the effect of atorvastatin on eNOS and Akt protein expression levels in HUVECs, cells were treated with 40μM, 10μM, 5μM, 1μM, 5nM, 2nM, 1nM atorvastatin under static condition.

Protein expression levels of eNOS were increased with atorvastatin treatment compared to the control group although these increases were not statistically significant ($p>0.05$) (Figure 4.6). This increase was highest, ~6-fold increase in 1 μM atorvastatin concentration compared to the control group, followed by a four-fold increase in the 5 μM group. (Figure 4.6)

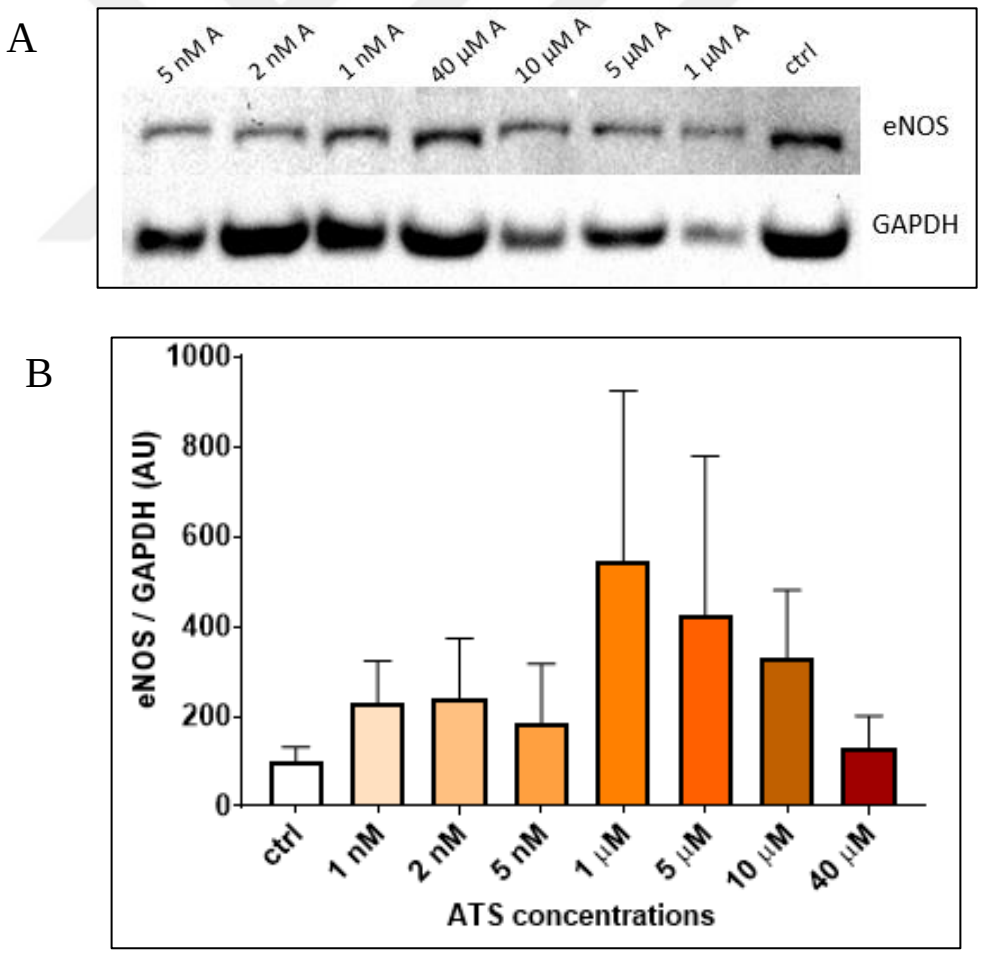

Figure 4.6. Effect of atorvastatin on eNOS protein expression levels in HUVECs. A) Representative western blot images of eNOS protein expression B) Average band intensity results (ctrl: control). For statistical analysis, Student's t-test was performed ($p>0.05$, $n=4$).

Akt protein expression levels were increased ~2-fold in 1 μM and 5 nM atorvastatin treated groups compared to the control group. (Figure 4.7)

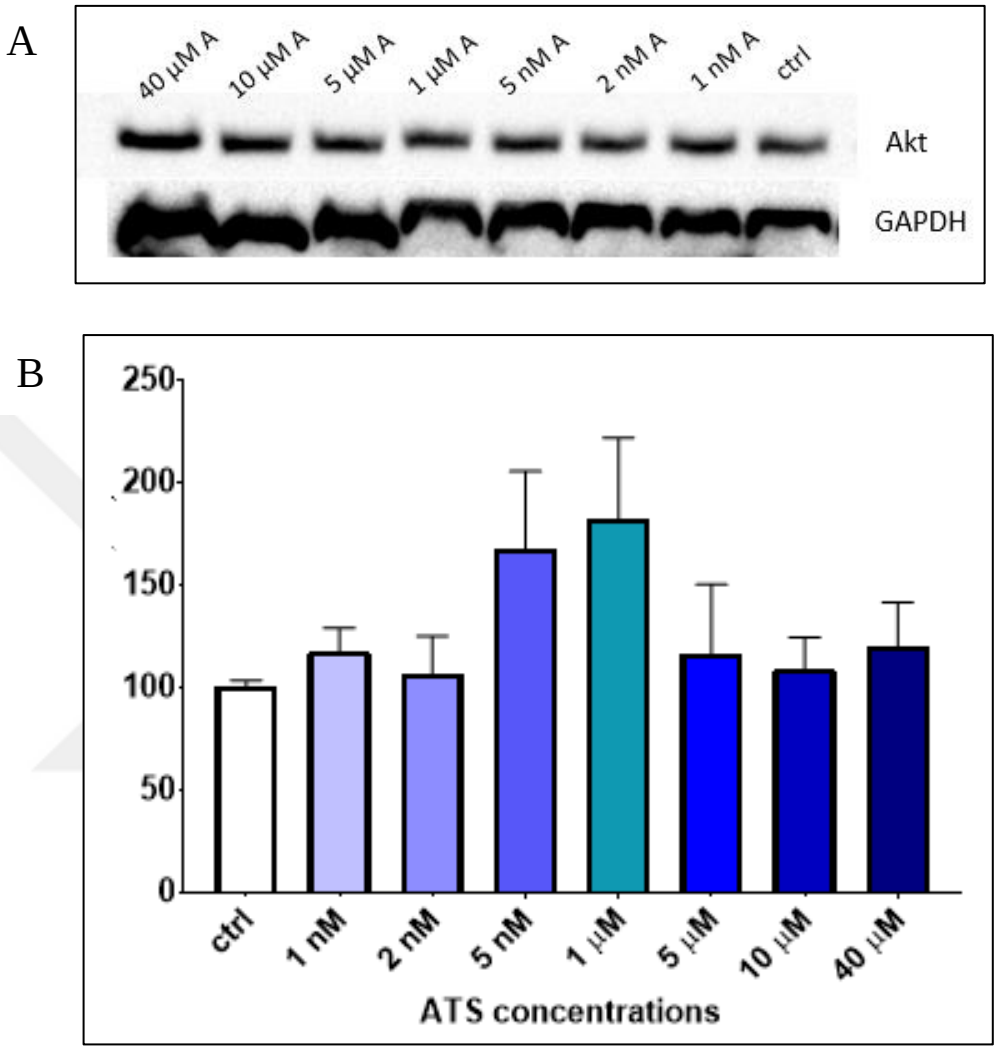

Figure 4.7. Effect of atorvastatin on Akt protein expression levels in HUVECs. A) Representative western blot images of Akt protein expression B) Average band intensity results (ctrl: control) For statistical analysis, Stud ent's t-test was performed. ($p>0.05$, $n=4$).

4.5. EFFECT OF ATS-APT-NP ON eNOS PROTEIN EXPRESSION LEVELS

In the present study to mimic atherosclerotic flow conditions, HUVECs were exposed to LOF. In order to demonstrate the effect of different flow conditions on the expression of eNOS protein levels were measured since eNOS is found to be decreased in the atherosclerotic area. Expression levels of eNOS protein were measured in HUVECs under NF and LOF conditions for 24 hours. Expression levels of eNOS protein were decreased approximately two-fold under LOF compared to the NF conditions, however, this effect was not statistically significant ($p>0.05$, Figure 4.8).

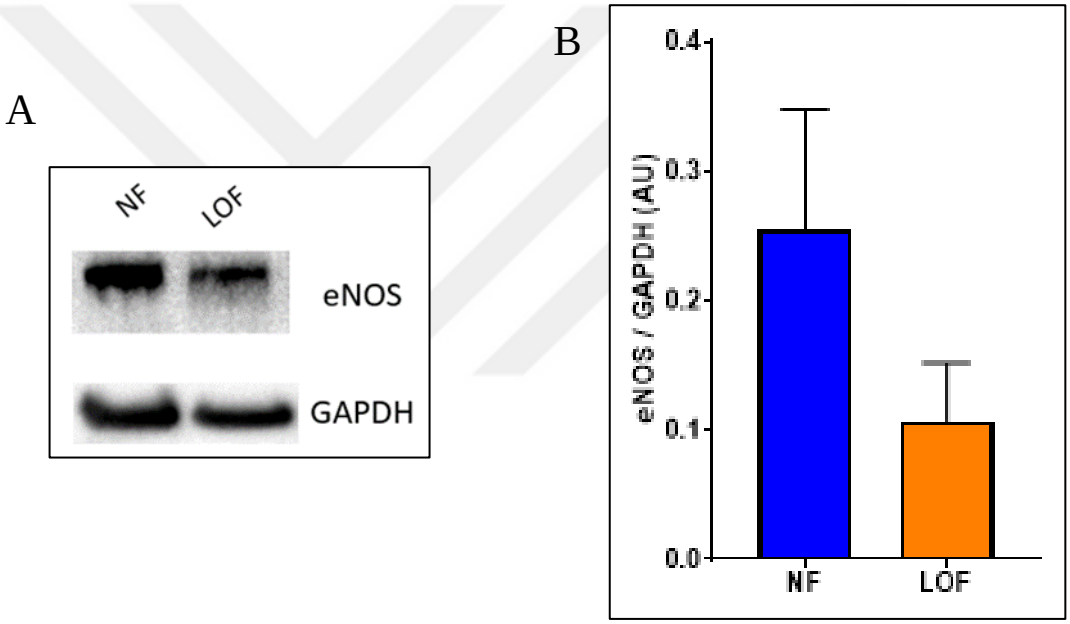

Figure 4.8. Effect of flow conditions on eNOS protein expression levels in HUVECs. A) Representative western blot images of eNOS protein expression B) Average band intensity results (NF: normal flow, LOF: low oscillating flow). For statistical analysis, Student's t-test was performed. ($p>0.05$, $n=3$)

Treatment of HUVECs under LOF conditions with 5 nM atorvastatin for 24 hours increased eNOS protein expression levels 4.3-fold compared to the control group while 1 nM and 2 nM atorvastatin increased eNOS protein expression levels 1.4 and 1.8 fold, respectively (Figure 4.9). On the other hand, 2 nM atorvastatin delivery by ATS-APT-NP increased eNOS protein expression levels ~1.4 fold compared to 2 nM atorvastatin treatment alone. In addition, 2 nM atorvastatin delivery by ATS-APT-NP increased eNOS protein expression

levels 2.6 fold compared to the control group. However, 1 nM and 5 nM atorvastatin delivery with ATS-APT-NP decreased eNOS protein expression by 2.9 and 5.4 fold respectively compared to atorvastatin treatment alone. (Figure 4.9).

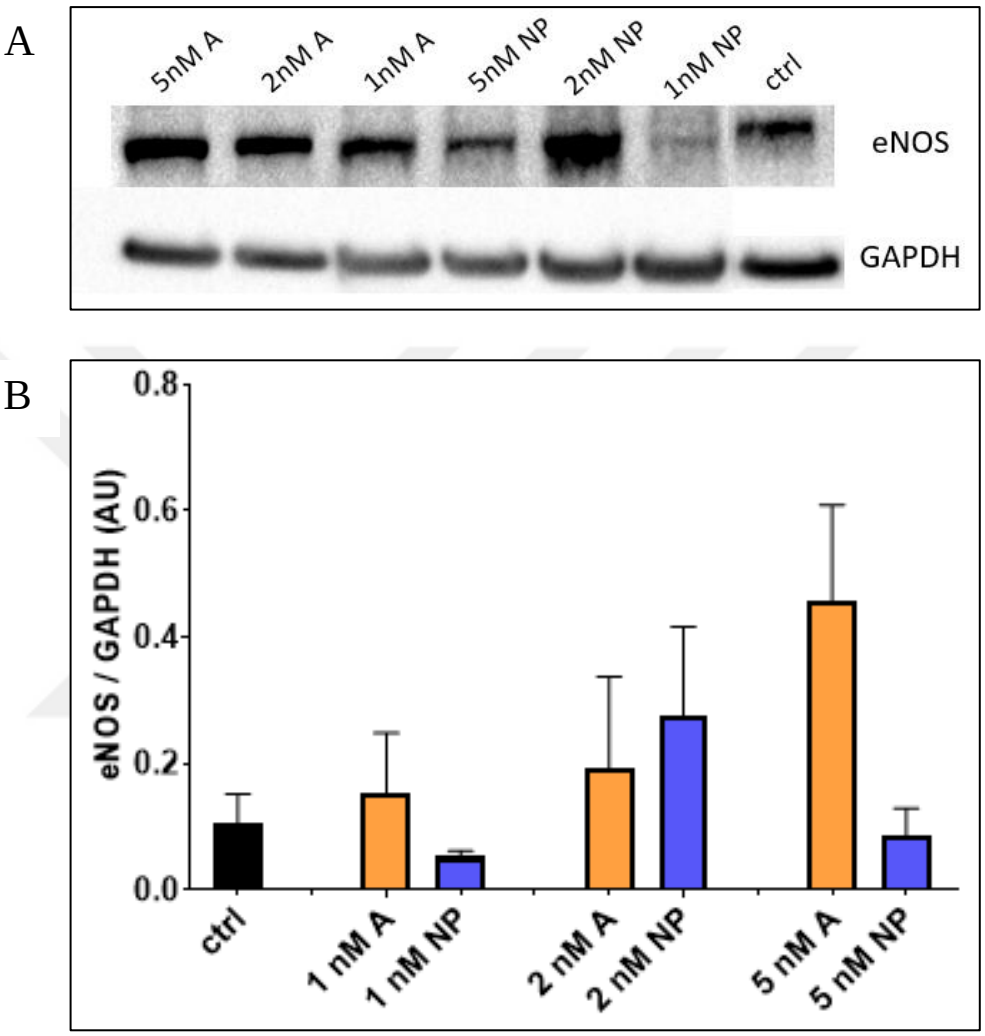

Figure 4.9. Effect of atorvastatin and ATS-APT-NP on eNOS protein expression levels in HUVECs under LOF conditions. ctrl: control, without any treatments; A: atorvastatin, NP: APT-ATS-NP. For statistical analysis, Student's t-test was performed. ($p>0.05$, $n=3$)

4.6. EFFECT OF ATS-APT-NP ON Akt PROTEIN EXPRESSION LEVELS

In the present study to mimic atherosclerotic flow conditions, HUVECs were exposed to LOF. In order to demonstrate the effect of different flow conditions on the expression of Akt protein levels was measured since Akt is an upstream pathway of eNOS. Expression levels

of Akt protein were measured in HUVECs under NF and LOF conditions for 24 hours. Akt protein expression was decreased 2.7 fold by LOF compared to NF (Figure 4.10.).

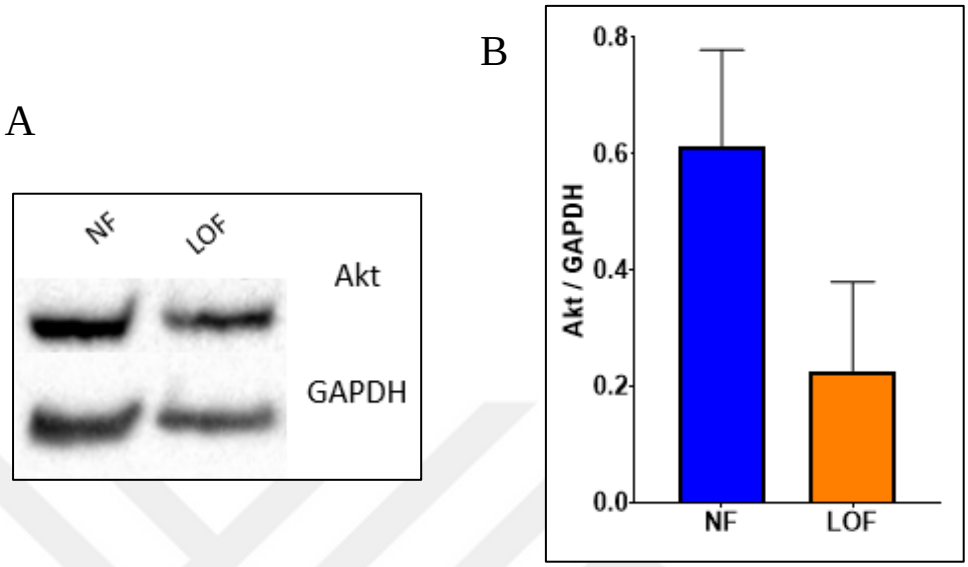

Figure 4.10. Effect of flow conditions on Akt protein expression levels in HUVECs. A) Representative western blot images of Akt protein expression B) Average band intensity results (NF: normal flow, LOF: low oscillating flow). For statistical analysis, Student's t-test was performed ($p>0.05$, $n=3$).

Treatment of HUVECs under LOF conditions with atorvastatin alone did not affect Akt protein expression compared to control. On the other hand, 2 nM and 5 nM atorvastatin delivery by ATS-APT-NP increased Akt protein expression levels 5.2 fold and 1.3 fold compared to only atorvastatin treatment, respectively (Figure 4.11 A, B). However, 1 nM atorvastatin delivery with ATS-APT-NP decreased Akt protein expression 2.9 fold compared to atorvastatin treatment alone (Figure 4.11 A, B).

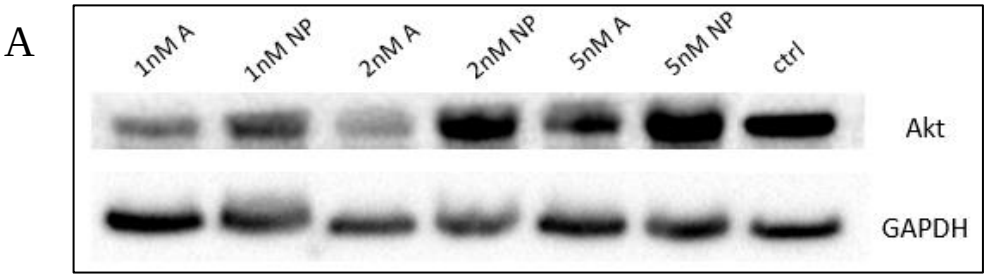

B

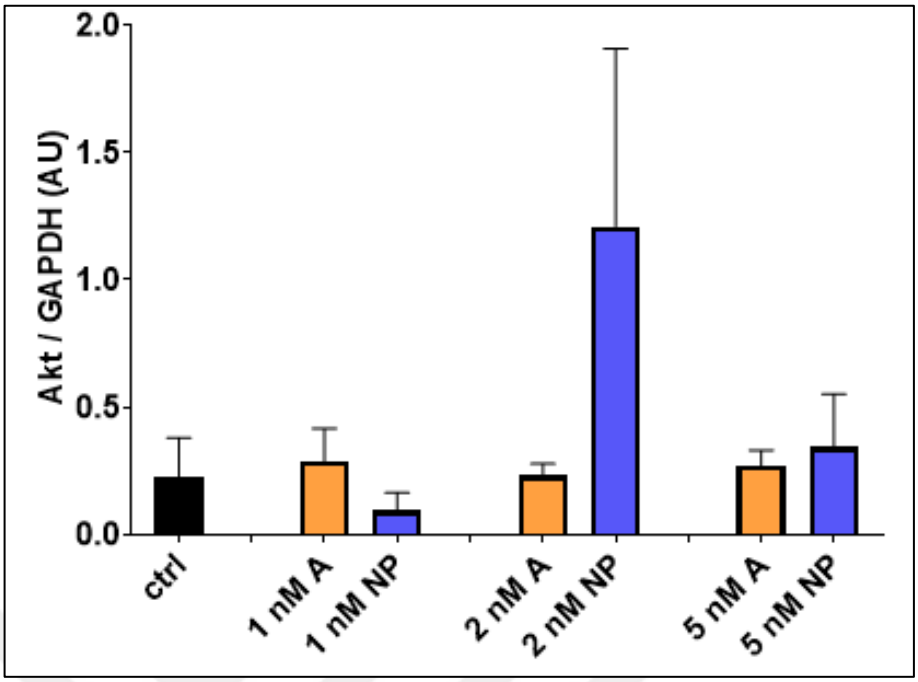

Figure 4.11. Effects of APT-ATS-NP on Akt protein expression levels in HUVECs under flow conditions. A) Representative western blot images of Akt protein expression B) Average band intensity results (ctrl: control, LOF not-treated). For statistical analysis, Student's t-test was performed ($p>0.05$, $n=3$).

4.7. EFFECT OF ATS-APT-NP ON eNOS PHOSPHORYLATION LEVELS

In the present study to mimic atherosclerotic flow conditions, HUVECs were exposed to LOF. In order to demonstrate the effect of different flow conditions on the expression of peNOS protein were measured since phosphorylation of eNOS is reported to increase its enzymatic activity. Expression levels of peNOS protein were measured in HUVECs under NF and LOF conditions for 24 hours. LOF condition resulted in a 2.8-fold increase in peNOS protein expression levels compared to the NF condition (Figure 4.12 A, B).

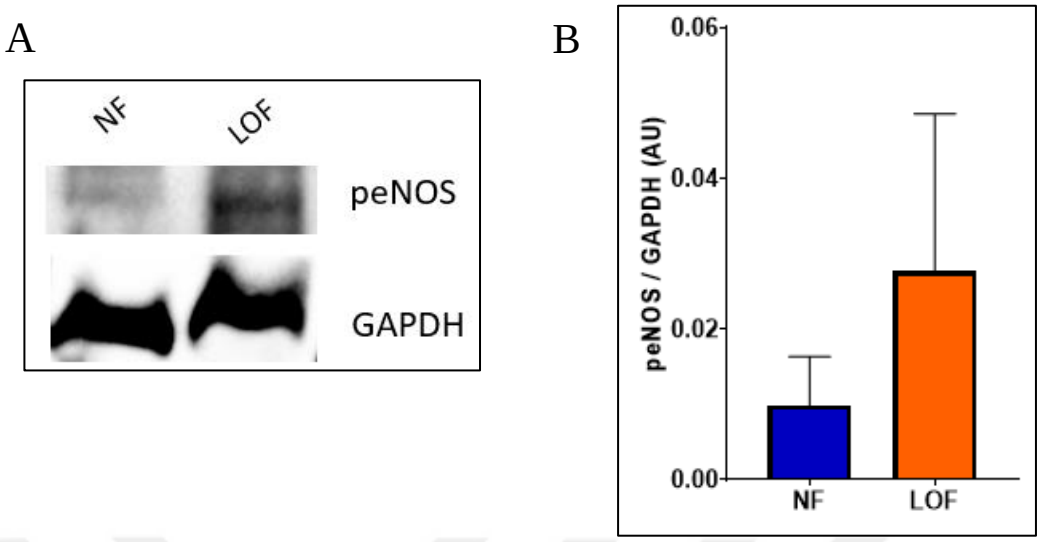

Figure 4.12. Effect of flow conditions on peNOS protein expression levels in HUVECs. A) Representative western blot images of peNOS protein expression B) Average band intensity results (NF: normal flow, LOF: low oscillating flow). For statistical analysis, Student's t-test was performed. ($p>0.05$, $n=3$).

Parallel with these results, the ratio of peNOS to total eNOS, which indicates the phosphorylation of the enzyme, was increased 3.3 fold by LOF compared to the NF condition (Figure 4.13).

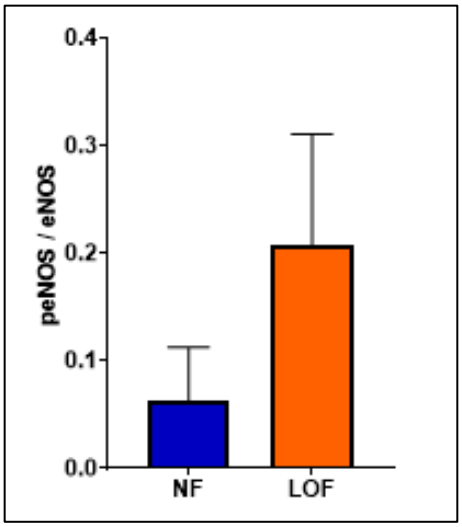

Figure 4.13. Effect of flow conditions on eNOS phosphorylation levels in HUVECs (NF: normal flow, LOF: low oscillating flow). For statistical analysis, Student's t-test was performed ($p>0.05$, $n=3$).

Treatment of HUVECs under LOF conditions with 1 nM and 5 nM atorvastatin increased peNOS protein expression levels 1.7 fold and 3.9 fold compared to control, respectively (Figure 4.14. A, B). 2 nM atorvastatin treatment of HUVECs under LOF conditions decreased peNOS protein expression levels 1.6 fold compared to control. However, 2 nM atorvastatin delivery by APT-ATS-NP increased the peNOS protein expression 1.6 fold compared to LOF and 2.7 fold compared to 2 nM atorvastatin treatment (Figure 4.14 A, B). On the other hand, 1 nM atorvastatin delivery with ATS-APT-NP decreased peNOS protein expression 1.3 fold compared to atorvastatin treatment alone (Figure 4.14 A, B).

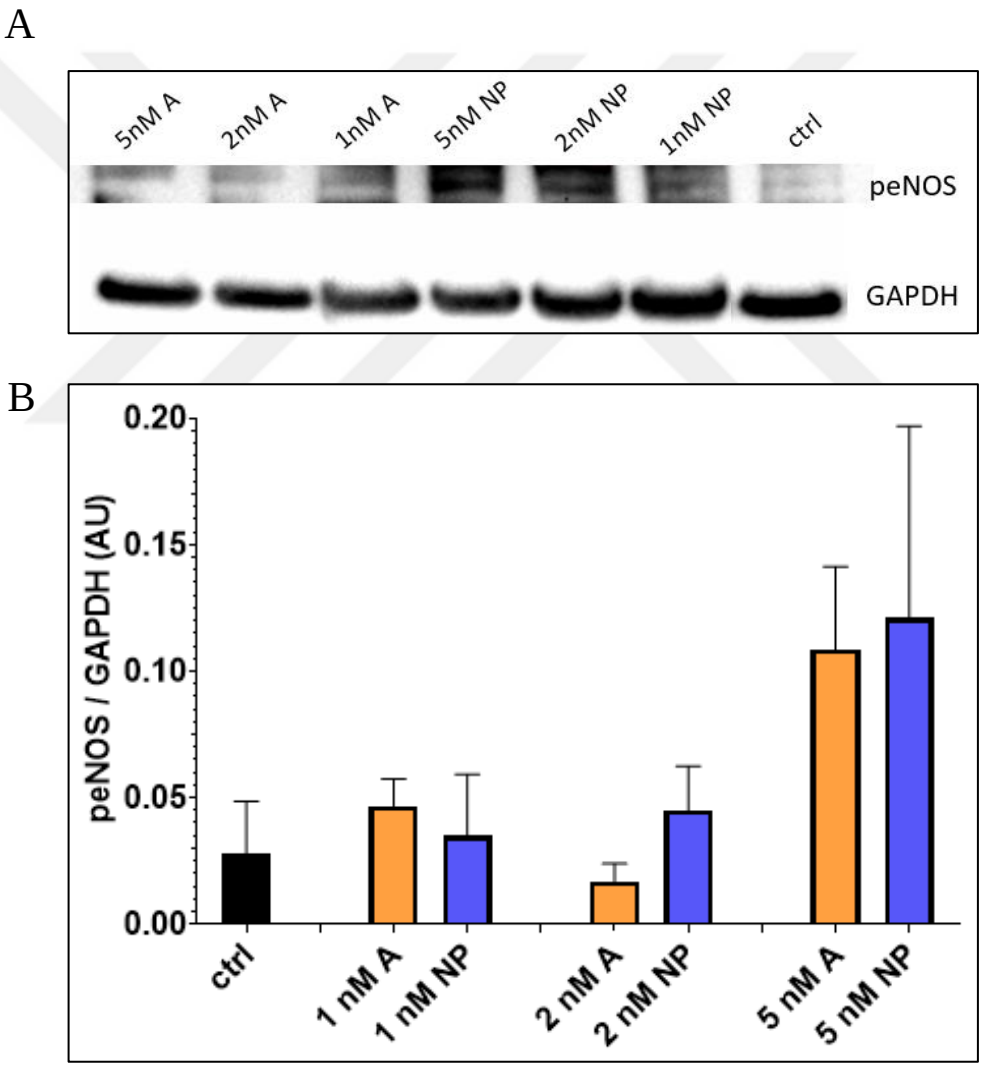

Figure 4.14. Effects of APT-ATS-NP on peNOS protein expression levels in HUVECs under flow conditions. A) Representative western blot images of peNOS protein expression B) Average band intensity results (ctrl: control, LOF not-treated). For statistical analysis, Student's t-test was performed. ($p>0.05$, $n=3$)

Treatment of HUVECs under LOF conditions with 5 nM atorvastatin increased phosphorylation of eNOS 75 fold compared to control and 42 fold compared to atorvastatin treatment alone (Figure 4.15). However, 1 nM atorvastatin delivery by APT-ATS-NP decreased phosphorylation of eNOS 3.8 fold compared to atorvastatin treatment (Figure 4.15).

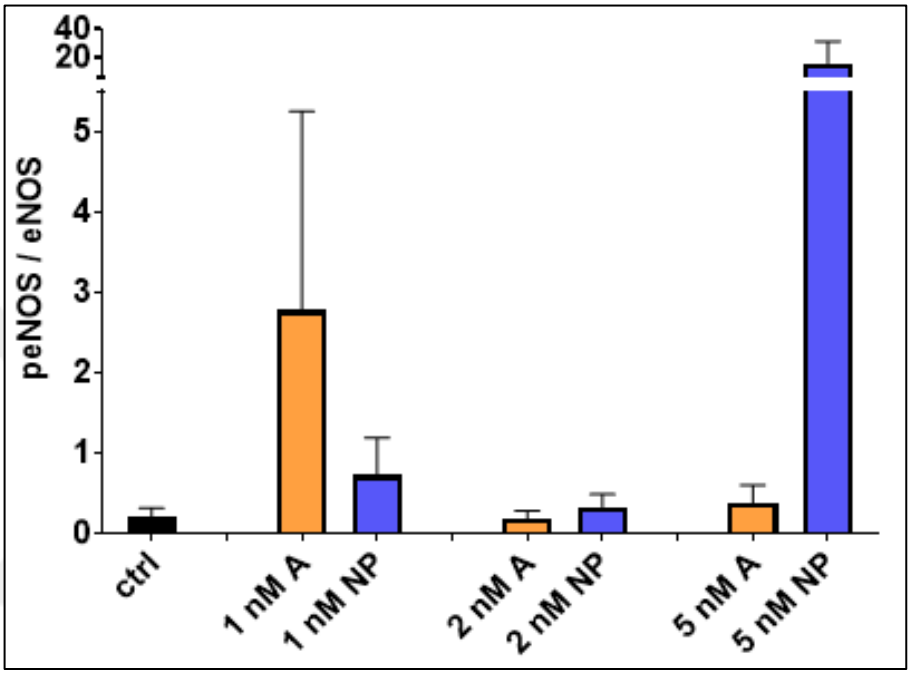

Figure 4.15. Effects of APT-ATS-NP on eNOS phosphorylation levels in HUVECs under flow conditions (ctrl: control, LOF not-treated). For statistical analysis, Student's t-test was performed. ($p>0.05$, $n=3$)

4.8. EFFECT OF ATS-APT-NP ON Akt PHOSPHORYLATION LEVELS

In the present study to mimic atherosclerotic flow conditions, HUVECs were exposed to LOF. In order to demonstrate the effect of different flow conditions on the expression of pAkt protein were measured since phosphorylation of Akt is reported to increase its enzymatic activity. Expression levels of pAkt protein were measured in HUVECs under NF and LOF conditions for 24 hours. LOF condition did not cause a change in pAkt protein expression levels compared to NF. (Figure 4.16)

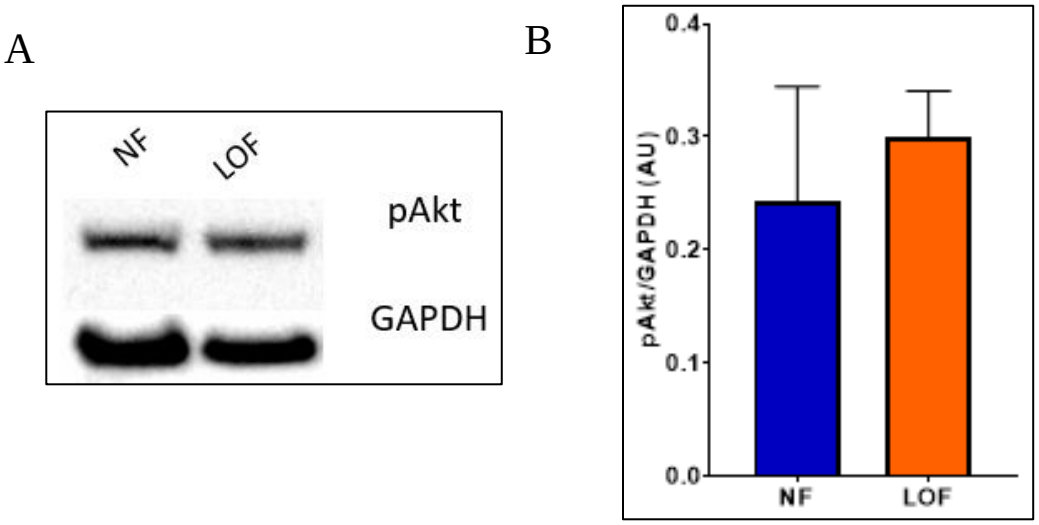

Figure 4.16. Effect of flow conditions on pAkt protein expression levels in HUVECs. A) Representative western blot images of peNOS protein expression B) Average band intensity results (NF: normal flow, LOF: low oscillating flow). For statistical analysis, Student's t-test was performed. ($p>0.05$, $n=3$)

On the other hand, the ratio of pAkt to total Akt, which indicates the phosphorylation of the enzyme, was increased 41-fold by LOF compared to NF conditions. (Figure 4.17)

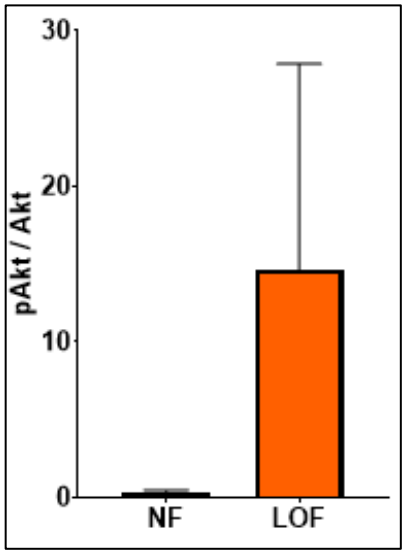

Figure 4.17. Effect of flow conditions on Akt phosphorylation levels in HUVECs (NF: normal flow, LOF: low oscillating flow). For statistical analysis, Student's t-test was performed ($p>0.05$, $n=3$).

On the other hand, 1 nM, 2nM, and 5 nM atorvastatin delivery by APT-ATS-NP increased the pAkt protein expression levels 2.2 fold, 2.1 fold ($p<0.05$), and 1.4 compared to control and 1.8, 1.6 and 1.4 compared to atorvastatin treatment, respectively (Figure 4.18A, B).

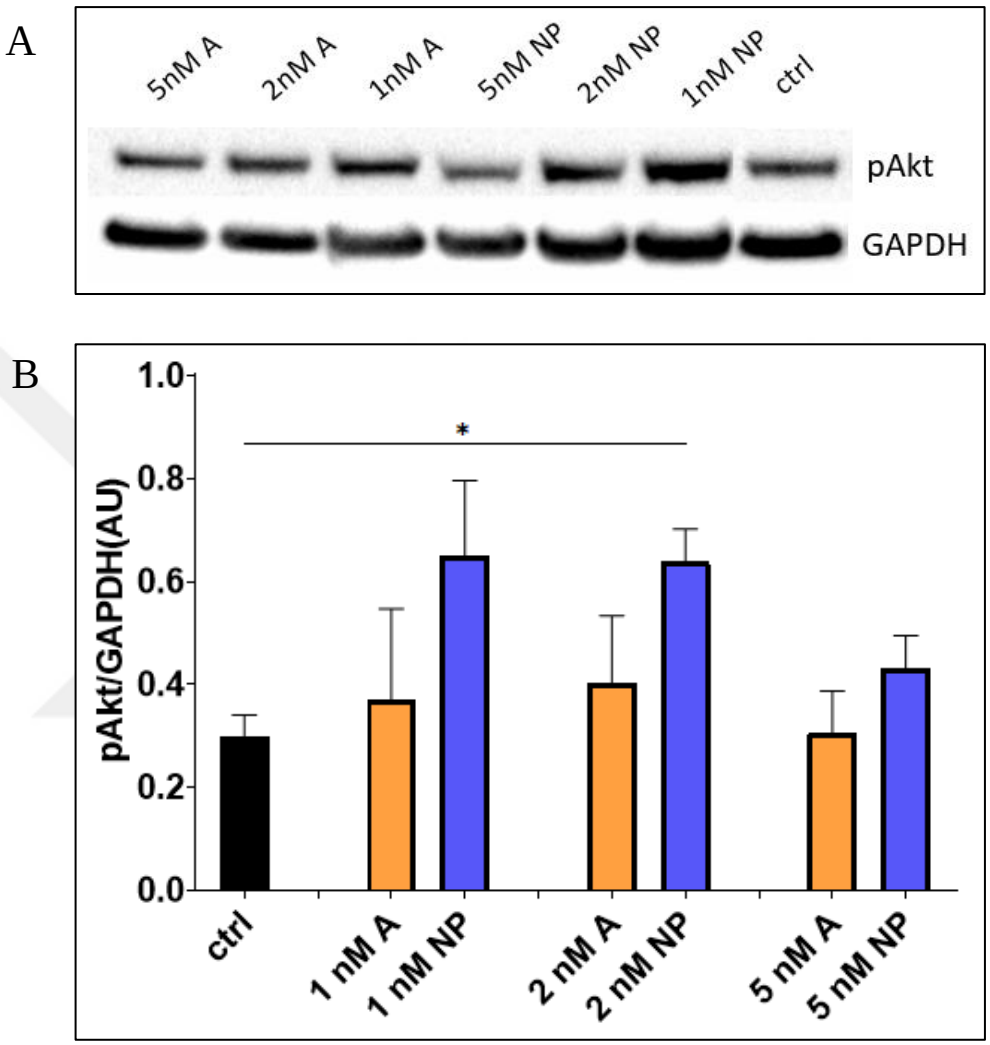

Figure 4.18. Effects of APT-ATS-NP on pAkt protein expression levels in HUVECs under flow conditions A) Representative western blot images of pAkt protein expression B) Average band intensity results (ctrl: control, LOF not-treated). For statistical analysis, Student's t-test was performed (*$p<0.05$, n=3).

1 nM atorvastatin delivery by APT-ATS-NP increased phosphorylation of Akt 2.9 fold compared to control and 17.7 fold compared to atorvastatin treatment alone (Figure 4.19). In addition, 5 nM atorvastatin delivery by APT-ATS-NP increased phosphorylation of Akt 7.9 fold compared to atorvastatin treatment alone (Figure 4.19).

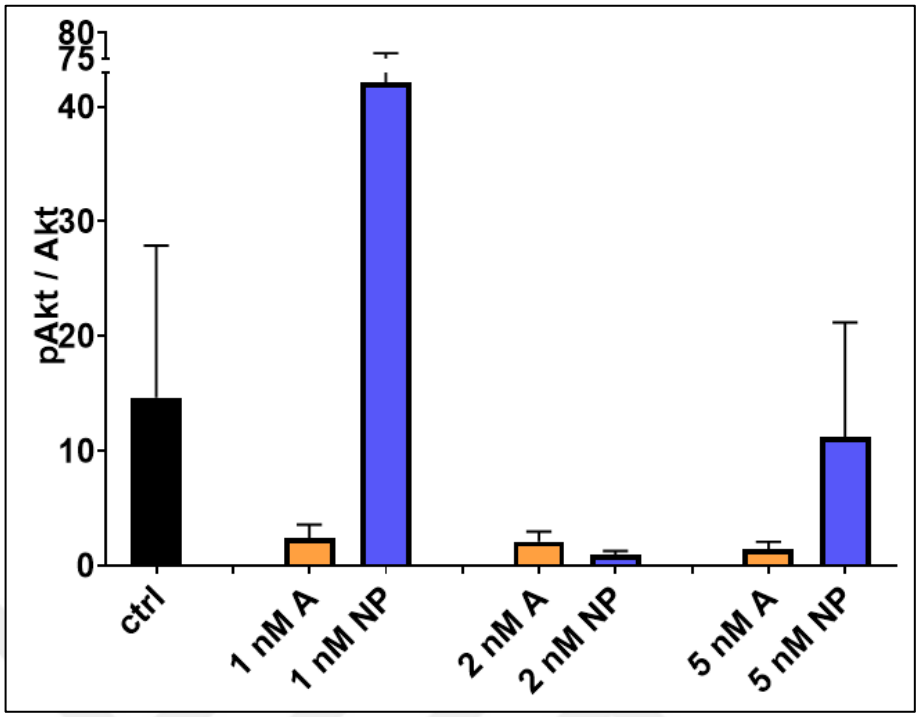

Figure 4.19. Effects of APT-ATS-NP on Akt phosphorylation levels in HUVECs under flow conditions. (ctrl: control, LOF not-treated). For statistical analysis, Student's t-test was performed ($p>0.05$, $n=3$).

5. DISCUSSION

In the present study, aptamer gated nanoparticles (APT-ATS-NP) were used as an alternative drug delivery system for efficient treatment of atherosclerosis specifically at pre-phase by targeting inflammation. The effects of atorvastatin delivery and its controlled release by APT-ATS-NP were investigated on shear stress-exposed HUVECs, a pre-atherosclerosis cell-culture model, and to evaluate its effectiveness intracellular ROS levels and eNOS/Akt proteins phosphorylation levels were measured. The results from the current study demonstrated that atorvastatin delivery by APT-ATS-NP significantly decreased intracellular ROS levels compared to atorvastatin treatment alone. Moreover, we measured that atorvastatin delivery by APT-ATS-NP increased the phosphorylation levels of the eNOS/Akt pathway compared to only atorvastatin treatment at low doses. Overall, targeting inflammation for the treatment of pre-atherosclerosis by aptamer gated nanoparticles might be a promising therapeutic approach.

Many medications are used with traditional pharmaceutical delivery methods, which are frequently linked to poor medical performance and efficacy due to their inability to target specific cells. Application of targeted drug delivery to lower systemic toxicity by using specified target sites such as organelles, cells, tissues, or organs has become a promising research breakthrough in recent years. In this context, a specialized targeting component, including an aptamer or an antibody, is commonly coupled or conjugated onto nanoparticles carrying drugs to create targeted delivery systems. Stable, low or non-immunogenic, accessible to surface changes, easily functionalized, and capable of site-specific delivery and secretion of encapsulated medicines solely at the target cellular locations are all desirable characteristics of a nanoparticle drug delivery system [100,111,144]. Even though enzymes and antibodies were used primarily for targeting specific sites, using aptamers for targeting has many advantages. For example, aptamers are similar to antibodies in term of their high affinity towards their targets. In addition, nucleic acid feature of aptamers is a big advantage that allows them to achieve structural changes and form “open” and “closed” forms. This molecular switching feature of aptamers applies to any aptamer sequence when a working targeted drug delivery design is achieved [143]. In addition, the controlled release of the drugs is an important factor to keep the concentration at a constant level for a longer duration in the desired area. There are many approaches to achieve controlled release of drugs by

capping the nanoparticles with materials that respond to stimuli such as PH, magnetic field, temperature, light, oxidation capabilities, and enzymatic activity [143]. In this context, a variety of options for drug delivery systems could be created by integrating the capabilities of aptamers including stimuli-responsive gates for drug loaded nanoparticles or molecular sensors [145]. Also, aptamer-based capping systems could produce favorable drug release kinetics at the intended target locations [146]. Therefore, aptamer gated silica nanoparticles were used in the present study. It was evaluated that ICAM-1 expression was increased by LOF conditions. In addition ICAM-1 was reported as an inflammatory biomarker in several studies [147,148]. These features make this protein a suitable target for drug delivery for atherosclerosis treatment in pre-atherosclerosis stage. Therefore, ICAM-1 aptamer was used as a gate in the present study.

Increased ROS is an important contributor and indicator of atherosclerotic plaque formation [56]. On the other hand, statin is a compound known for its effect on decreasing ROS [149]. Therefore, in the present study, intracellular ROS levels were measured to evaluate the effectiveness of atorvastatin delivery by APT-ATS-NP to HUVECs under atherosclerosis mimicking shear stress conditions. In this context, many studies demonstrated elevated antioxidant ad reduced ROS levels due to statin treatments in humans, rodents, and cell culture [56]. For example, a study conducted with chronic heart failure patients indicated that atorvastatin treatment of 20 mg/day for 8 weeks resulted in a significant increase in activity of both extracellular and erythrocyte superoxide dismutase (SOD), a fundamental antioxidant mechanism in the vasculature, compared to both control and placebo group [150]. In the same study, it has been reported that plasma malondialdehyde (MDA), a marker of oxidative stress, was significantly decreased compared to the control group [151]. In another study by Pignatelli *et al*., the mechanism behind the antioxidant effect of atorvastatin was investigated by treating hypercholesterolemia patients with atorvastatin (40mg/day) along with a Mediterranean diet [152]. In that study, serum oxidative stress was assessed by measuring the levels of NOX2, a ROS-generating enzyme and it was reported that two hours after atorvastatin administration serum NOX2 levels and NOX2 activation were significantly reduced [152].

In the literature, although there are numerous studies about the roles of statins on ROS levels in atherosclerosis, there only few studies which reports the usage of nanoparticles in this context. In the current study, the concertation of atorvastatin used was 0.1 mM which was

decided after intensive search of literature in this area of research. For example, in clinical practices patients are treated with statins in the range of 10 to 80 mg per day, therefore maximum treatment with statins refers to 0.5 to 1.6 mg/kg dose for patients with weight range of 50–150 kg. In mice this concentration refers to approximately 7–20 mg/kg dose for mouse. [153]. On the other hand, in a study with $Apoe^{-/-}$ mice, a high dose of atorvastatin (100 mg/kg) was used since long-term low dosage treatment of atorvastatin may cause anti-inflammatory and stabilizing effects on atherosclerotic lesions and could cover the anti-oxidant effect of the drug [153]. It has been elucidated that a high dosage of atorvastatin treatment (100 mg/kg) significantly decreased both extracellular and intracellular ROS levels of the aortic arch of $Apoe^{-/-}$ mice [153]. In the present study, 0.1 mM atorvastatin treatment was applied to HUVECs with or without APT-ATS-NP under atherosclerosis mimicking flow conditions. Results revealed a significant decrease in intracellular ROS levels of APT-ATS-NP applied cells compared to atorvastatin treatment alone. Similar to our findings, in the study by Gao *et al.*, ROS-responsive nanoparticles which were used in the concentration of 0.4 mm as a targeted drug delivery system revealed a reduction in intracellular ROS levels in inflammation-induced macrophages when atorvastatin is delivered via nanoparticles compared to only atorvastatin treatment alone, even though this effect was not significant [154]. In conclusion, in the present study, it was elucidated that atorvastatin delivery by APT-ATS-NP is significantly more efficient compared to only atorvastatin treatment in the context of decreasing ROS in the HUVECs under atherosclerosis mimicking conditions.

Moreover, in the present study, the effects of APT-ATS-NP on the Akt/eNOS signaling pathway under atherosclerosis mimicking shear stress conditions were investigated, since one of the pleiotropic effects of atorvastatin are increasing eNOS levels and NO bioavailability . On the other hand, one of the main advantages of targeted drug delivery is decreasing the systematically given dosage of a drug. Therefore, in the present study, firstly the effects of different concentrations of atorvastatin (1 nM to 40 μM) on eNOS and Akt protein expression levels in HUVECs under static conditions were determined. 1 nM atorvastatin and above increased eNOS protein expression levels with the highest level measured at 10 μM atorvastatin treatment in HUVECs. Parallel with these results, 1 nM atorvastatin treatment caused an increase in Akt protein expression levels in HUVECs.

Therefore; 1 nM, 2 nM, and 5 nM concentration of atorvastatin treatment was applied to cells in the rest of the study.

In the present study, atherosclerosis mimicking conditions (LOF) decreased the protein expression levels of both eNOS and Akt. These findings are similar with the literature in the sense of considering high laminar shear stress as atheroprotective and low disturbed/oscillating shear stress as atheroprone [15]. For example, in the study of Ghimire *et al.* HUVECs were exposed to high laminar shear stress (10 dyn/cm^2) which is considered to create atheroprotective state. In that study, it was evaluated that eNOS expression of cells under flow conditions was higher than in static conditions [155]. On the other hand, in the present study phosphorylation levels of eNOS and Akt were found to be higher in atherosclerotic conditions than in the normal flow conditions which might be caused by the increasing need for NO in the shear stress-exposed cells.

It has been elucidated in the present study that atorvastatin delivery by APT-ATS-NP has increased eNOS protein expression levels at 2 nM concentration compared to both control and atorvastatin treatment alone. Atorvastatin delivery by APT-ATS-NP was more effective than control in the context of eNOS phosphorylation levels in a low concentration as 2 nM. It should be noticed that these concentration is at least 3-5 times lower than those used in the literature. For example in the study of Feron *et al.* HUVECs were treated with 10 nM to 10 μM atorvastatin and no difference was observed in eNOS protein expression by the treatment with atorvastatin up to 1 μM [156]. In another study, 6.6 μM atorvastatin treatment induced eNOS mRNA expression levels in HUVECs [157]. Parallel with these results, in a study with H_2O_2-induced HUVECs atorvastatin treatment increased in eNOS protein expression levels in a dose-dependent manner with 10, 30 nM, or 0.1 μM concentrations [158].

Statins are known to regulate the pI3K/Akt pathway, which is an upstream pathway of eNOS signaling [158]. Therefore in the present study, to have an understanding of the underlying mechanism of eNOS phosphoryaltion via atorvastatin delivery by APT-ATS-NP, Akt protein expression and phosphorylation levels were investigated. Parallel with eNOS protein expression results, Akt was increased by atorvastatin delivery with APT-ATS-NP compared to both control and atorvastatin treatment alone at 2 nM concentration. In the study of Minami *et al.* 10 μM atorvastatin treatment on HUVECs caused a significant increase pAkt to total Akt ratio [159]. In another study with ischemic rats, 10 mg/kg/day of atorvastatin treatment caused a significant increase in pAkt/Akt ratio compared to the control group

[160]. In the study of Ota *et al.,* H_2O_2-induced HUVECs were treated with 100 nM atorvastatin, subsequently, an increase in the phosphorylation of Akt at the Ser-473 site was evaluated [158]. In the present study, phosphorylation of Akt (pAkt/Akt) was increased in HUVECs under atherosclerosis mimicking shear stress conditions with 1 nM atorvastatin delivery by APT-ATS-NP compared to atorvastatin treatment alone, which is an effect achieved by a lower concentration than literature. Therefore, it could be suggested that atorvastatin delivery by APT-ATS-NP is more effective than atorvastatin treatment alone in the context of Akt activation, an upstream pathway of eNOS signaling.

Finally, present study demonstrates that atorvastatin delivery by aptamer gated silica nanoparticles is more effective than control in the sense of decreasing intracellular ROS levels, increasing eNOS and Akt protein expression and activation of eNOS/Akt pathway on the HUVECs under atherosclerosis mimicking shear stress conditions. These results make APT-ATS-NP a potential targeted drug delivery system for the treatment of shear stress-exposed endothelial dysfunction and subsequently for the treatment of atherosclerosis.

6. CONCLUSION

Atherosclerotic cardiovascular diseases, one of the main causes of death worldwide, certainly pose a serious risk for human health. Atherosclerosis is currently treated systemically rather than locally, which causes lower efficacy and increased side effects. Although basic research and application studies are still in early phases, substantial advancements have been made in both areas, which raises the prospect of nanoparticle technology's diagnostic and therapeutic applications in atherosclerosis. On the other hand, inflammation is an important step of pre-atherosclerosis and for that reason it is a promising target for preventive treatment by targeted drug delivery systems. In this context, in the present study, pre-atherosclerotic conditions mimicked by low sear stress exposure to HUVECs and nanoparticles that target an inflammatory biomarker, ICAM-1, delivered the atorvastatin to the area for the treatment of atherosclerosis in the early stages. Therefore, ICAM-1 aptamer gated atorvastatin-loaded silica nanoparticles were used to treat the shear stress-exposed HUVECs. Results indicated lower intracellular ROS levels when atorvastatin was delivered by APT-ATS-NP compared to the control group in shear stress-exposed HUVECs. Moreover, the application of atorvastatin in shear stress-exposed HUVECs resulted in higher phosphorylation levels of the Akt/eNOS pathway when delivered by APT-ATS-NP compared to control in concentration as low as 5 nM which is a lower concentration than the previous studies that achieve this effect in the literature. However, it should be noticed that these experiments were done with a limited number of trials. Thus, future studies with more trials and preferably including in vivo animal studies has to be done. Also, these experiments should be repeated with other statins like rosuvastatin or simvastatin to show that the findings obtained in this study are not specific to atorvastatin.

Finally, to fully understand the molecular mechanism of targeted atorvastatin delivery by aptamer conjugated nanoparticles as a treatment for atherosclerosis further research is needed to be conducted in more detail.

REFERENCES

1. Kumar V, Abbas AK, Aster JC. Robbins Basic Pathology, 10th edition. 2018. 361–378 p.

2. The Global Burden of Disease Study 2017 (GBD 2017) [Internet]. Institute for Health Metrics and Evaluation (IHME), University of Washington. 2017. Available from: http://ghdx.healthdata.org/gbd-results-tool

3. Şahin B, İlgün G. Risk factors of deaths related to cardiovascular diseases in World Health Organization (WHO) member countries. Health Soc Care Community. 2020 Sep 9;n/a(n/a).

4. Pahwa R, Jialal I. Atherosclerosis [Internet]. StatPearls. 2020. Available from: https://www.ncbi.nlm.nih.gov/books/NBK507799/

5. Roth GA, Johnson C, Abajobir A, Abd-Allah F, Abera SF, Abyu G, et al. Global, Regional, and National Burden of Cardiovascular Diseases for 10 Causes, 1990 to 2015. J Am Coll Cardiol. 2017/05/17. 2017 Jul 4;70(1):1–25.

6. Haybar H, Shahrabi S, Rezaeeyan H, Shirzad R, Saki N. Endothelial Cells: From Dysfunction Mechanism to Pharmacological Effect in Cardiovascular Disease. Cardiovasc Toxicol. 2019 Feb 1;19(1):13–22.

7. Lawson C, Wolf S. ICAM-1 signaling in endothelial cells. Pharmacol Reports. 2009 Jan;61(1):22–32.

8. Malek AM. Hemodynamic Shear Stress and Its Role in Atherosclerosis. JAMA. 1999 Dec 1;282(21):2035.

9. Duchene J, Cayla C, Vessillier S, Scotland R, Yamashiro K, Lecomte F, et al. Laminar shear stress regulates endothelial kinin B1 receptor expression and function: potential implication in atherogenesis. Arterioscler Thromb Vasc Biol. 2009 Nov;29(11):1757–63.

10. Roux E, Bougaran P, Dufourcq P, Couffinhal T. Fluid Shear Stress Sensing by the Endothelial Layer. Front Physiol. 2020;11(July):1–17.

11. Morbiducci U, Kok AM, Kwak BR, Stone PH, Steinman DA, Wentzel JJ. Atherosclerosis at arterial bifurcations: Evidence for the role of haemodynamics and geometry. Thromb Haemost. 2016;115(3):484–92.

12. Fung Y-C. Biomechanics. New York, NY: Springer New York; 1993.

13. Paszkowiak JJ, Dardik A. Arterial Wall Shear Stress: Observations from the Bench to the Bedside. Vasc Endovascular Surg. 2003 Jan 19;37(1):47–57.

14. Kumar S, Maxwell IZ, Heisterkamp A, Polte TR, Lele TP, Salanga M, et al. Viscoelastic retraction of single living stress fibers and its impact on cell shape, cytoskeletal organization, and extracellular matrix mechanics. Biophys J. 2006 May 15;90(10):3762–73.

15. Heo K-S, Fujiwara K, Abe J. Shear stress and atherosclerosis. Mol Cells. 2014/04/30. 2014 Jun;37(6):435–40.

16. Sakamoto N, Ueki Y, Oi M, Kiuchi T, Sato M. Fluid shear stress suppresses ICAM-1-mediated transendothelial migration of leukocytes in coculture model. Biochem Biophys Res Commun. 2018 Jul;502(3):403–8.

17. Nagel T, Resnick N, Atkinson WJ, Dewey CF, Gimbrone MA. Shear stress selectively upregulates intercellular adhesion molecule-1 expression in cultured human vascular endothelial cells. J Clin Invest. 1994 Aug 1;94(2):885–91.

18. Meza D, Shanmugavelayudam SK, Mendoza A, Sanchez C, Rubenstein DA, Yin W. Platelets modulate endothelial cell response to dynamic shear stress through PECAM-1. Thromb Res. 2017 Feb;150:44–50.

19. Martin-Ventura J, Rodrigues-Diez R, Martinez-Lopez D, Salaices M, Blanco-Colio L, Briones A. Oxidative Stress in Human Atherothrombosis: Sources, Markers and Therapeutic Targets. Int J Mol Sci. 2017 Nov 3;18(11):2315.

20. Forstermann U, Sessa WC. Nitric oxide synthases: regulation and function. Eur Heart J. 2012 Apr 1;33(7):829–37.

21. Chen J, Ye Z, Wang X, Chang J, Yang M, Zhong H, et al. Nitric oxide bioavailability dysfunction involves in atherosclerosis. Biomed Pharmacother. 2018 Jan;97:423–8.

22. Mónica FZ, Bian K, Murad F. Chapter One - The Endothelium-Dependent Nitric Oxide–cGMP Pathway. In: Khalil RABT-A in P, editor. Endothelium. Academic Press; 2016. p. 1–27.

23. Carvajal JA, Germain AM, Huidobro-Toro JP, Weiner CP. Molecular mechanism of cGMP-mediated smooth muscle relaxation. J Cell Physiol. 2000 Sep;184(3):409–20.

24. Dou D, Zheng X, Ying L, Ye L, Gao Y. Sulfhydryl-dependent Dimerization and cGMP-mediated Vasodilatation. J Cardiovasc Pharmacol. 2013 Jul;62(1):1–5.

25. Förstermann U. Oxidative stress in vascular disease: causes, defense mechanisms and potential therapies. Nat Clin Pract Cardiovasc Med. 2008 Jun 6;5(6):338–49.

26. Bohlen HG. Nitric Oxide and the Cardiovascular System. In: Comprehensive Physiology. Wiley; 2015. p. 803–28.

27. Stuehr DJ, Haque MM. Nitric oxide synthase enzymology in the 20 years after the Nobel Prize. Br J Pharmacol. 2019 Jan 9;176(2):177–88.

28. Stuehr DJ, Haque MM. Nitric oxide synthase enzymology in the 20 years after the Nobel Prize. Br J Pharmacol. 2019;176(2):177–88.

29. Hong F fang, Liang X yu, Liu W, Lv S, He S jin, Kuang H bin, et al. Roles of eNOS in atherosclerosis treatment. Inflamm Res. 2019;68(6):429–41.

30. Izumi Y, Clifford DB, Zorumski CF. Inhibition of Long-Term Potentiation by NMDA-Mediated Nitric Oxide Release. Science (80-). 1992 Aug 28;257(5074):1273–6.

31. Togashi H, Sakuma I, Yoshioka M, Kobayashi T, Yasuda H, Kitabatake A, et al. A central nervous system action of nitric oxide in blood pressure regulation. J Pharmacol Exp Ther. 1992 Jul;262(1):343–7.

32. Förstermann U, Closs EI, Pollock JS, Nakane M, Schwarz P, Gath I, et al. Nitric oxide synthase isozymes. Characterization, purification, molecular cloning, and functions. Hypertension. 1994 Jun;23(6_pt_2):1121–31.

33. Rajfer J, Aronson WJ, Bush PA, Dorey FJ, Ignarro LJ. Nitric Oxide as a Mediator of Relaxation of the Corpus Cavernosum in Response to Nonadrenergic, Noncholinergic

Neurotransmission. N Engl J Med. 1992 Jan 9;326(2):90–4.

34. Schwarz PM, Kleinert H, Förstermann U. Potential Functional Significance of Brain-Type and Muscle-Type Nitric Oxide Synthase I Expressed in Adventitia and Media of Rat Aorta. Arterioscler Thromb Vasc Biol. 1999 Nov;19(11):2584–90.

35. Nathan CF, Hibbs JB. Role of nitric oxide synthesis in macrophage antimicrobial activity. Curr Opin Immunol. 1991 Jan;3(1):65–70.

36. Fehsel K, Jalowy A, Qi S, Burkart V, Hartmann B, Kolb H. Islet Cell DNA Is a Target of Inflammatory Attack by Nitric Oxide. Diabetes. 1993 Mar 1;42(3):496–500.

37. Langrehr JM, Hoffman RA, Billiar TR, Lee KK, Schraut WH, Simmons RL. Nitric oxide synthesis in the in vivo allograft response: a possible regulatory mechanism. Surgery. 1991 Aug;110(2):335–42.

38. Lange M. Role of nitric oxide in shock: the large animal perspective. Front Biosci. 2009;Volume(14):1979.

39. Alderton WK, Cooper CE, Knowles RG. Nitric oxide synthases: Structure, function and inhibition. Biochem J. 2001;357(3):593–615.

40. Hong F, Liang X, Liu W, Lv S, He S, Kuang H, et al. Roles of eNOS in atherosclerosis treatment. Inflamm Res. 2019 Jun 1;68(6):429–41.

41. Herranz B, Marquez S, Guijarro B, Aracil E, Aicart-Ramos C, Rodriguez-Crespo I, et al. Integrin-linked kinase regulates vasomotor function by preventing endothelial nitric oxide synthase uncoupling: role in atherosclerosis. Circ Res. 2012 Feb 3;110(3):439–49.

42. Margaritis M, Antonopoulos AS, Digby J, Lee R, Reilly S, Coutinho P, et al. Interactions Between Vascular Wall and Perivascular Adipose Tissue Reveal Novel Roles for Adiponectin in the Regulation of Endothelial Nitric Oxide Synthase Function in Human Vessels. Circulation. 2013 Jun 4;127(22):2209–21.

43. Chen Z-P, Mitchelhill KI, Michell BJ, Stapleton D, Rodriguez-Crespo I, Witters LA, et al. AMP-activated protein kinase phosphorylation of endothelial NO synthase. FEBS Lett. 1999 Jan 29;443(3):285–9.

44. Michell BJ, Harris MB, Chen Z, Ju H, Venema VJ, Blackstone MA, et al. Identification of Regulatory Sites of Phosphorylation of the Bovine Endothelial Nitric-oxide Synthase at Serine 617 and Serine 635. J Biol Chem. 2002 Nov;277(44):42344–51.

45. Lane P, Gross SS. Disabling a C-terminal Autoinhibitory Control Element in Endothelial Nitric-oxide Synthase by Phosphorylation Provides a Molecular Explanation for Activation of Vascular NO Synthesis by Diverse Physiological Stimuli. J Biol Chem. 2002 May;277(21):19087–94.

46. Mount PF, Kemp BE, Power DA. Regulation of endothelial and myocardial NO synthesis by multi-site eNOS phosphorylation. J Mol Cell Cardiol. 2007 Feb;42(2):271–9.

47. Lubrano V, Balzan S. LOX-1 and ROS, inseparable factors in the process of endothelial damage. Free Radic Res. 2014 Aug 23;48(8):841–8.

48. Vanhoutte PM, Shimokawa H, Feletou M, Tang EHC. Endothelial dysfunction and vascular disease - a 30th anniversary update. Acta Physiol. 2017 Jan;219(1):22–96.

49. Fleming I, Fisslthaler B, Dixit M, Busse R. Role of PECAM-1 in the shear-stress-induced activation of Akt and the endothelial nitric oxide synthase (eNOS) in endothelial cells. J Cell Sci. 2005;118(18):4103–11.

50. Hu Y, Chen M, Wang M, Li X. Flow-mediated vasodilation through mechanosensitive G protein-coupled receptors in endothelial cells. Trends Cardiovasc Med. 2021;(xxxx).

51. Revathidevi S, Munirajan AK. Akt in cancer: Mediator and more. Semin Cancer Biol. 2019 Dec;59:80–91.

52. Fulton D, Gratton J-P, McCabe TJ, Fontana J, Fujio Y, Walsh K, et al. Regulation of endothelium-derived nitric oxide production by the protein kinase Akt. Nature. 1999 Jun 10;399(6736):597–601.

53. Dimmeler S, Assmus B, Hermann C, Haendeler J, Zeiher AM. Fluid Shear Stress Stimulates Phosphorylation of Akt in Human Endothelial Cells. Circ Res. 1998 Aug 10;83(3):334–41.

54. Dimmeler S, Fleming I, Fisslthaler B, Hermann C, Busse R, Zeiher AM. Activation of nitric oxide synthase in endothelial cells by Akt-dependent phosphorylation. Nature. 1999 Jun;399(6736):601–5.

55. Stocker R, Keaney JF. Role of Oxidative Modifications in Atherosclerosis. Physiol Rev. 2004 Oct;84(4):1381–478.

56. Förstermann U, Xia N, Li H. Roles of Vascular Oxidative Stress and Nitric Oxide in the Pathogenesis of Atherosclerosis. Circ Res. 2017 Feb 17;120(4):713–35.

57. Li H, Horke S, Förstermann U. Vascular oxidative stress, nitric oxide and atherosclerosis. Atherosclerosis. 2014 Nov;237(1):208–19.

58. Sheehan AL, Carrell S, Johnson B, Stanic B, Banfi B, Miller FJ. Role for Nox1 NADPH oxidase in atherosclerosis. Atherosclerosis. 2011 Jun;216(2):321–6.

59. Douglas G, Bendall JK, Crabtree MJ, Tatham AL, Carter EE, Hale AB, et al. Endothelial-specific Nox2 overexpression increases vascular superoxide and macrophage recruitment in ApoE−/− mice. Cardiovasc Res. 2012 Apr 1;94(1):20–9.

60. Vendrov AE, Hakim ZS, Madamanchi NR, Rojas M, Madamanchi C, Runge MS. Atherosclerosis Is Attenuated by Limiting Superoxide Generation in Both Macrophages and Vessel Wall Cells. Arterioscler Thromb Vasc Biol. 2007 Dec;27(12):2714–21.

61. Patetsios P, Song M, Shutze WP, Pappas C, Rodino W, Ramirez JA, et al. Identification of uric acid and xanthine oxidase in atherosclerotic plaque11This study was supported by a grant from the Committee on Research Allocation, Department of Surgery, State University of New York Health Science Center at Brooklyn, Brooklyn, New. Am J Cardiol. 2001 Jul;88(2):188–91.

62. Guzik TJ, Sadowski J, Guzik B, Jopek A, Kapelak B, Przybyłowski P, et al. Coronary Artery Superoxide Production and Nox Isoform Expression in Human Coronary Artery Disease. Arterioscler Thromb Vasc Biol. 2006 Feb;26(2):333–9.

63. Schröder K, Vecchione C, Jung O, Schreiber JG, Shiri-Sverdlov R, van Gorp PJ, et al. Xanthine oxidase inhibitor tungsten prevents the development of atherosclerosis in ApoE knockout mice fed a Western-type diet. Free Radic Biol Med. 2006

Nov;41(9):1353–60.

64. Nomura J, Busso N, Ives A, Matsui C, Tsujimoto S, Shirakura T, et al. Xanthine Oxidase Inhibition by Febuxostat Attenuates Experimental Atherosclerosis in Mice. Sci Rep. 2015 May 1;4(1):4554.

65. Ballinger SW, Patterson C, Knight-Lozano CA, Burow DL, Conklin CA, Hu Z, et al. Mitochondrial Integrity and Function in Atherogenesis. Circulation. 2002 Jul 30;106(5):544–9.

66. Xia N, Daiber A, Habermeier A, Closs EI, Thum T, Spanier G, et al. Resveratrol Reverses Endothelial Nitric-Oxide Synthase Uncoupling in Apolipoprotein E Knockout Mice. J Pharmacol Exp Ther. 2010 Oct;335(1):149–54.

67. Alp NJ, McAteer MA, Khoo J, Choudhury RP, Channon KM. Increased Endothelial Tetrahydrobiopterin Synthesis by Targeted Transgenic GTP-Cyclohydrolase I Overexpression Reduces Endothelial Dysfunction and Atherosclerosis in ApoE-Knockout Mice. Arterioscler Thromb Vasc Biol. 2004 Mar;24(3):445–50.

68. Kattoor AJ, Pothineni NVK, Palagiri D, Mehta JL. Oxidative Stress in Atherosclerosis. Curr Atheroscler Rep. 2017 Nov 18;19(11):42.

69. Pacher P, Beckman JS, Liaudet L. Nitric Oxide and Peroxynitrite in Health and Disease. Physiol Rev. 2007 Jan;87(1):315–424.

70. Weber C, Noels H. Atherosclerosis: current pathogenesis and therapeutic options. Nat Med. 2011 Nov 7;17(11):1410–22.

71. Peter Libby MD PhD, Robert O. Bonow MD MS, Douglas L. Mann MD, Gordon F Tomaselli MD, Deepak Bhatt MD MPH FACC FAHA FSCAI FESC, Scott D. Solomon MD EBMMSF. Braunwald’s Heart Disease-A Textbook of Cardiovascular Medicine. 12th ed. Elsevier Inc.; 2022.

72. Libby P. The changing landscape of atherosclerosis. Nature. 2021 Apr 22;592(7855):524–33.

73. Alonso R, Cuevas A, Cafferata A. Diagnosis and Management of Statin Intolerance. J Atheroscler Thromb. 2019 Mar 1;26(3):207–15.

74. Sirtori CR. The pharmacology of statins. Pharmacol Res. 2014 Oct;88:3–11.

75. Almeida SO, Budoff M. Effect of statins on atherosclerotic plaque. Trends Cardiovasc Med. 2019 Nov;29(8):451–5.

76. PEDERSEN TR. Randomised trial of cholesterol lowering in 4444 patients with coronary heart disease: the Scandinavian Simvastatin Survival Study (4S). Atheroscler Suppl. 2004 Oct;5(3):81–7.

77. Meor Anuar Shuhaili MFR, Samsudin IN, Stanslas J, Hasan S, Thambiah SC. Effects of Different Types of Statins on Lipid Profile: A Perspective on Asians. Int J Endocrinol Metab. 2017 Apr 22;In Press(In Press).

78. Endo A. Drugs inhibiting HMG-CoA reductase. Pharmacol Ther. 1985;31(3):257–67.

79. Malinowski JM. Atorvastatin: A hydroxymethylglutaryl-coenzyme A reductase inhibitor. Am J Heal Pharm. 1998 Nov 1;55(21):2253–67.

80. Clarke AT, Mills PR. Atorvastatin associated liver disease. Dig Liver Dis. 2006 Oct;38(10):772–7.

81. Blum CB. Comparison of properties of four inhibitors of 3-hydroxy-3-methylglutaryl-coenzyme a reductase. Am J Cardiol. 1994 May;73(14):D3–11.

82. Adhyaru BB, Jacobson TA. Safety and efficacy of statin therapy. Nat Rev Cardiol. 2018 Dec 30;15(12):757–69.

83. Ridker PM, Danielson E, Fonseca FAH, Genest J, Gotto AM, Kastelein JJP, et al. Rosuvastatin to Prevent Vascular Events in Men and Women with Elevated C-Reactive Protein. N Engl J Med. 2008 Nov 20;359(21):2195–207.

84. High-Dose Atorvastatin after Stroke or Transient Ischemic Attack. N Engl J Med. 2006 Aug 10;355(6):549–59.

85. Wierzbicki AS. Atorvastatin. Expert Opin Pharmacother. 2001 May 24;2(5):819–30.

86. van Leuven SI, Kastelein JJ. Atorvastatin. Expert Opin Pharmacother. 2005 Jun 15;6(7):1191–203.

87. Taylor AJ, Kent SM, Flaherty PJ, Coyle LC, Markwood TT, Vernalis MN. ARBITER: Arterial Biology for the Investigation of the Treatment Effects of Reducing Cholesterol. Circulation. 2002 Oct 15;106(16):2055–60.

88. Andrews TC, Ballantyne CM, Hsia JA, Kramer JH. Achieving and maintaining national cholesterol education program low-density lipoprotein cholesterol goals with five statins. Am J Med. 2001 Aug;111(3):185–91.

89. Smilde T, van Wissen S, Awollersheim H, Trip M, Kastelein J, Stalenhoef A. Effect of aggressive versus conventional lipid lowering on atherosclerosis progression in familial hypercholesterolemia (ASAP): a prospective, randomised, double-blind trial. Lancet. 2001 Feb;357(9256):577–81.

90. Gorabi AM, Kiaie N, Hajighasemi S, Banach M, Penson PE, Jamialahmadi T, et al. Statin-Induced Nitric Oxide Signaling: Mechanisms and Therapeutic Implications. J Clin Med. 2019;8(12):2051.

91. Mehta JL, Li DY, Chen HJ, Joseph J, Romeo F. Inhibition of LOX-1 by Statins May Relate to Upregulation of eNOS. Biochem Biophys Res Commun. 2001 Dec;289(4):857–61.

92. Rikitake Y, Liao JK. Rho GTPases, Statins, and Nitric Oxide. Circ Res. 2005 Dec 9;97(12):1232–5.

93. Laufs U, Endres M, Custodis F, Gertz K, Nickenig G, Liao JK, et al. Suppression of Endothelial Nitric Oxide Production After Withdrawal of Statin Treatment Is Mediated by Negative Feedback Regulation of Rho GTPase Gene Transcription. Circulation. 2000 Dec 19;102(25):3104–10.

94. Wolfrum S, Dendorfer A, Rikitake Y, Stalker TJ, Gong Y, Scalia R, et al. Inhibition of Rho-Kinase Leads to Rapid Activation of Phosphatidylinositol 3-Kinase/Protein Kinase Akt and Cardiovascular Protection. Arterioscler Thromb Vasc Biol. 2004 Oct;24(10):1842–7.

95. Davignon J, Jacob RF, Mason RP. The antioxidant effects of statins. Coron Artery Dis. 2004 Aug;15(5):251–8.

96. Moon GJ, Kim SJ, Cho YH, Ryoo S, Bang OY. Antioxidant Effects of Statins in

Patients with Atherosclerotic Cerebrovascular Disease. J Clin Neurol. 2014;10(2):140.

97. Tong H, Zhang X, Meng X, Lu L, Mai D, Qu S. Simvastatin Inhibits Activation of NADPH Oxidase/p38 MAPK Pathway and Enhances Expression of Antioxidant Protein in Parkinson Disease Models. Front Mol Neurosci. 2018 May 22;11.

98. Wassmann S, Laufs U, Bäumer AT, Müller K, Konkol C, Sauer H, et al. Inhibition of Geranylgeranylation Reduces Angiotensin II-Mediated Free Radical Production in Vascular Smooth Muscle Cells: Involvement of Angiotensin AT1 Receptor Expression and Rac1 GTPase. Mol Pharmacol. 2001 Mar 1;59(3):646–54.

99. Devarajan P V., Jain S, editors. Targeted Drug Delivery : Concepts and Design. Cham: Springer International Publishing; 2015. (Advances in Delivery Science and Technology).

100. Öztürk-Atar K, Eroğlu H, Çalış S. Novel advances in targeted drug delivery. J Drug Target. 2018 Sep 14;26(8):633–42.

101. Strebhardt K, Ullrich A. Paul Ehrlich's magic bullet concept: 100 years of progress. Nat Rev Cancer. 2008 Jun 12;8(6):473–80.

102. Kleinstreuer C, Basciano CA, Childress EM, Kennedy AS. A New Catheter for Tumor Targeting With Radioactive Microspheres in Representative Hepatic Artery Systems. Part I: Impact of Catheter Presence on Local Blood Flow and Microsphere Delivery. J Biomech Eng. 2012 May 1;134(5).

103. Childress EM, Kleinstreuer C, Kennedy AS. A New Catheter for Tumor-Targeting With Radioactive Microspheres in Representative Hepatic Artery Systems—Part II: Solid Tumor-Targeting in a Patient-Inspired Hepatic Artery System. J Biomech Eng. 2012 May 1;134(5).

104. Dunaevsky A. The Gene-Gun Approach for Transfection and Labeling of Cells in Brain Slices. In 2013. p. 111–8.

105. Mishra P, Nayak B, Dey RK. PEGylation in anti-cancer therapy: An overview. Asian J Pharm Sci. 2016;11(3):337–48.

106. Garnett MC. Targeted drug conjugates: principles and progress. Adv Drug Deliv Rev. 2001 Dec;53(2):171–216.

107. Mahato R, Tai W, Cheng K. Prodrugs for improving tumor targetability and efficiency. Adv Drug Deliv Rev. 2011 Jul;63(8):659–70.

108. Torchilin V. Nanoparticulates as drug carriers. Imperial college press, London, UK. 2006.

109. Scott RC, Rosano JM, Ivanov Z, Wang B, Chong PL-G, Issekutz AC, et al. Targeting VEGF-encapsulated immunoliposomes to MI heart improves vascularity and cardiac function. FASEB J. 2009 Oct 1;23(10):3361–7.

110. Dvir T, Bauer M, Schroeder A, Tsui JH, Anderson DG, Langer R, et al. Nanoparticles Targeting the Infarcted Heart. Nano Lett. 2011 Oct 12;11(10):4411–4.

111. Ambesh P, Campia U, Obiagwu C, Bansal R, Shetty V, Hollander G, et al. Nanomedicine in coronary artery disease. Indian Heart J. 2017;69(2):244–51.

112. Lewis DR, Petersen LK, York AW, Zablocki KR, Joseph LB, Kholodovych V, et al. Sugar-based amphiphilic nanoparticles arrest atherosclerosis in vivo. Proc Natl Acad Sci. 2015 Mar 3;112(9):2693 LP – 2698.

113. Lobatto ME, Fayad ZA, Silvera S, Vucic E, Calcagno C, Mani V, et al. Multimodal Clinical Imaging To Longitudinally Assess a Nanomedical Anti-Inflammatory Treatment in Experimental Atherosclerosis. Mol Pharm. 2010 Dec 6;7(6):2020–9.

114. Broz P, Ben-Haim N, Grzelakowski M, Marsch S, Meier W, Hunziker P. Inhibition of Macrophage Phagocytotic Activity by a Receptor-targeted Polymer Vesicle-based Drug Delivery Formulation of Pravastatin. J Cardiovasc Pharmacol. 2008 Mar;51(3):246–52.

115. Katsuki S, Matoba T, Nakashiro S, Sato K, Koga J, Nakano K, et al. Nanoparticle-Mediated Delivery of Pitavastatin Inhibits Atherosclerotic Plaque Destabilization/Rupture in Mice by Regulating the Recruitment of Inflammatory Monocytes. Circulation. 2014 Feb 25;129(8):896–906.

116. Nakashiro S, Matoba T, Umezu R, Koga J, Tokutome M, Katsuki S, et al.

Pioglitazone-Incorporated Nanoparticles Prevent Plaque Destabilization and Rupture by Regulating Monocyte/Macrophage Differentiation in ApoE −/− Mice. Arterioscler Thromb Vasc Biol. 2016 Mar;36(3):491–500.

117. Winter PM, Neubauer AM, Caruthers SD, Harris TD, Robertson JD, Williams TA, et al. Endothelial α ν β 3 Integrin–Targeted Fumagillin Nanoparticles Inhibit Angiogenesis in Atherosclerosis. Arterioscler Thromb Vasc Biol. 2006 Sep;26(9):2103–9.

118. Bhowmick T, Berk E, Cui X, Muzykantov VR, Muro S. Effect of flow on endothelial endocytosis of nanocarriers targeted to ICAM-1. J Control Release. 2012 Feb;157(3):485–92.

119. Cicha I. Strategies to enhance nanoparticle-endothelial interactions under flow. J Cell Biotechnol. 2016 May 12;1(2):191–208.

120. Reynolds PR, Larkman DJ, Haskard DO, Hajnal J V., Kennea NL, George AJT, et al. Detection of Vascular Expression of E-selectin in Vivo with MR Imaging. Radiology. 2006 Nov;241(2):469–76.

121. Zhu Q, Liu G, Kai M. DNA Aptamers in the Diagnosis and Treatment of Human Diseases. Vol. 20, Molecules . 2015.

122. Tuerk C, Gold L. Systematic evolution of ligands by exponential enrichment: RNA ligands to bacteriophage T4 DNA polymerase. Science (80-). 1990 Aug 3;249(4968):505 LP – 510.

123. Bayat P, Nosrati R, Alibolandi M, Rafatpanah H, Abnous K, Khedri M, et al. SELEX methods on the road to protein targeting with nucleic acid aptamers. Biochimie. 2018 Nov;154:132–55.

124. Ali MH, Elsherbiny ME, Emara M. Updates on aptamer research. Int J Mol Sci. 2019;20(10):1–23.

125. Şener BB, Yiğit D, Bayraç AT, Bayraç C. Inhibition of cell migration and invasion by ICAM-1 binding DNA aptamers. Anal Biochem. 2021 Sep;628:114262.

126. Dursun AD, Dogan S, Kavruk M, Busra Tasbasi B, Sudagidan M, Deniz Yilmaz M,

et al. Surface plasmon resonance aptasensor for soluble ICAM-1 protein in blood samples. Analyst. 2022;147(8):1663–8.

127. Sola M, Menon AP, Moreno B, Meraviglia-Crivelli D, Soldevilla MM, Cartón-García F, et al. Aptamers Against Live Targets: Is In Vivo SELEX Finally Coming to the Edge? Mol Ther - Nucleic Acids. 2020 Sep;21:192–204.

128. Mi J, Liu Y, Rabbani ZN, Yang Z, Urban JH, Sullenger BA, et al. In vivo selection of tumor-targeting RNA motifs. Nat Chem Biol. 2010 Jan 29;6(1):22–4.

129. Huang R-H, Fremont DH, Diener JL, Schaub RG, Sadler JE. A Structural Explanation for the Antithrombotic Activity of ARC1172, a DNA Aptamer that Binds von Willebrand Factor Domain A1. Structure. 2009 Nov;17(11):1476–84.

130. Wang P, Yang Y, Hong H, Zhang Y, Cai W, Fang D. Aptamers as Therapeutics in Cardiovascular Diseases. Curr Med Chem. 2011 Sep 1;18(27):4169–74.

131. Dyke CK, Steinhubl SR, Kleiman NS, Cannon RO, Aberle LG, Lin M, et al. First-in-Human Experience of an Antidote-Controlled Anticoagulant Using RNA Aptamer Technology. Circulation. 2006 Dec 5;114(23):2490–7.

132. Tan KX, Pan S, Jeevanandam J, Danquah MK. Cardiovascular therapies utilizing targeted delivery of nanomedicines and aptamers. Int J Pharm. 2019 Mar;558:413–25.

133. Narayan R, Nayak U, Raichur A, Garg S. Mesoporous Silica Nanoparticles: A Comprehensive Review on Synthesis and Recent Advances. Pharmaceutics. 2018 Aug 6;10(3):118.

134. Paris JL, Vallet-Regí M. Mesoporous Silica Nanoparticles for Co-Delivery of Drugs and Nucleic Acids in Oncology: A Review. Pharmaceutics. 2020 Jun 8;12(6).

135. Zhang Q, Wang X, Li P-Z, Nguyen KT, Wang X-J, Luo Z, et al. Biocompatible, Uniform, and Redispersible Mesoporous Silica Nanoparticles for Cancer-Targeted Drug Delivery In Vivo. Adv Funct Mater. 2014 May 1;24(17):2450–61.

136. Chen L, She X, Wang T, He L, Shigdar S, Duan W, et al. Overcoming acquired drug resistance in colorectal cancer cells by targeted delivery of 5-FU with EGF grafted

hollow mesoporous silica nanoparticles. Nanoscale. 2015;7(33):14080–92.

137. Peng X, Liang Y, Yin Y, Liao H, Li L. Development of a hollow mesoporous silica nanoparticles vaccine to protect against house dust mite induced allergic inflammation. Int J Pharm. 2018 Oct;549(1–2):115–23.

138. Mora-Raimundo P, Lozano D, Manzano M, Vallet-Regí M. Nanoparticles to Knockdown Osteoporosis-Related Gene and Promote Osteogenic Marker Expression for Osteoporosis Treatment. ACS Nano. 2019 May 28;13(5):5451–64.

139. Hernandez FJ, Hernandez LI, Pinto A, Schäfer T, Özalp VC. Targeting cancer cells with controlled release nanocapsules based on a single aptamer. Chem Commun. 2013;49(13):1285.

140. Kavruk M, Celikbicak O, Ozalp VC, Borsa BA, Hernandez FJ, Bayramoglu G, et al. Antibiotic loaded nanocapsules functionalized with aptamer gates for targeted destruction of pathogens. Chem Commun. 2015;51(40):8492–5.

141. Tuna BG, Atalay PB, Kuku G, Acar EE, Kara HK, Yilmaz MD, et al. Enhanced antitumor activity of carbendazim on HeLa cervical cancer cells by aptamer mediated controlled release. RSC Adv. 2019;9(62):36005–10.

142. Hernandez FJ, Hernandez LI, Kavruk M, Arıca YM, Bayramoğlu G, Borsa BA, et al. NanoKeepers: stimuli responsive nanocapsules for programmed specific targeting and drug delivery. Chem Commun. 2014;50(67):9489–92.

143. Ozalp VC, Eyidogan F, Oktem HA. Aptamer-Gated Nanoparticles for Smart Drug Delivery. Pharmaceuticals. 2011 Aug 15;4(8):1137–57.

144. Taneja G, Sud A, Pendse N, Panigrahi B, Kumar A, Sharma AK. Nano-medicine and Vascular Endothelial Dysfunction: Options and Delivery Strategies. Cardiovasc Toxicol. 2019;19(1):1–12.

145. Mairal T, Cengiz Özalp V, Lozano Sánchez P, Mir M, Katakis I, O'Sullivan CK. Aptamers: molecular tools for analytical applications. Anal Bioanal Chem. 2008 Feb 21;390(4):989–1007.

146. Chiu T-C, Huang C-C. Aptamer-Functionalized Nano-Biosensors. Sensors. 2009 Dec

21;9(12):10356–88.

147. Bui TM, Wiesolek HL, Sumagin R. ICAM-1: A master regulator of cellular responses in inflammation, injury resolution, and tumorigenesis. J Leukoc Biol. 2020;108(3):787–99.

148. Witkowska A. Soluble ICAM-1: A marker of vascular inflammation and lifestyle. Cytokine. 2005 Jul 21;31(2):127–34.

149. Hermida N, Balligand J-L. Low-Density Lipoprotein-Cholesterol-Induced Endothelial Dysfunction and Oxidative Stress: The Role of Statins. Antioxid Redox Signal. 2014 Mar 10;20(8):1216–37.

150. Pignatelli P, Carnevale R, Di Santo S, Bartimoccia S, Nocella C, Vicario T, et al. Rosuvastatin reduces platelet recruitment by inhibiting NADPH oxidase activation. Biochem Pharmacol. 2012 Dec;84(12):1635–42.

151. Castro PF, Miranda R, Verdejo HE, Greig D, Gabrielli LA, Alcaino H, et al. Pleiotropic Effects of Atorvastatin in Heart Failure: Role in Oxidative Stress, Inflammation, Endothelial Function, and Exercise Capacity. J Hear Lung Transplant. 2008 Apr;27(4):435–41.

152. Pignatelli P, Carnevale R, Pastori D, Cangemi R, Napoleone L, Bartimoccia S, et al. Immediate Antioxidant and Antiplatelet Effect of Atorvastatin via Inhibition of Nox2. Circulation. 2012 Jul 3;126(1):92–103.

153. Ekstrand M, Gustafsson Trajkovska M, Perman-Sundelin J, Fogelstrand P, Adiels M, Johansson M, et al. Imaging of Intracellular and Extracellular ROS Levels in Atherosclerotic Mouse Aortas Ex Vivo: Effects of Lipid Lowering by Diet or Atorvastatin. Gracia-Sancho J, editor. PLoS One. 2015 Jun 22;10(6):e0130898.

154. Gao C, Huang Q, Liu C, Kwong CHT, Yue L, Wan J-B, et al. Treatment of atherosclerosis by macrophage-biomimetic nanoparticles via targeted pharmacotherapy and sequestration of proinflammatory cytokines. Nat Commun. 2020 Dec 26;11(1):2622.

155. Ghimire K, Zaric J, Alday-Parejo B, Seebach J, Bousquenaud M, Stalin J, et al. MAGI1 Mediates eNOS Activation and NO Production in Endothelial Cells in

Response to Fluid Shear Stress. Vol. 8, Cells . 2019.

156. Feron O, Dessy C, Desager J-P, Balligand J-L. Hydroxy-Methylglutaryl–Coenzyme A Reductase Inhibition Promotes Endothelial Nitric Oxide Synthase Activation Through a Decrease in Caveolin Abundance. Circulation. 2001 Jan 2;103(1):113–8.

157. Morikawa S, Takabe W, Mataki C, Kanke T, Itoh T, Wada Y, et al. The Effect of Statins on mRNA Levels of Genes Related to Inflammation, Coagulation, and Vascular Constriction in HUVEC. J Atheroscler Thromb. 2002;9(4):178–83.

158. Ota H, Eto M, Kano MR, Kahyo T, Setou M, Ogawa S, et al. Induction of Endothelial Nitric Oxide Synthase, SIRT1, and Catalase by Statins Inhibits Endothelial Senescence Through the Akt Pathway. Arterioscler Thromb Vasc Biol. 2010 Nov;30(11):2205–11.

159. Minami T, Satoh K, Nogi M, Kudo S, Miyata S, Tanaka S, et al. Statins up-regulate SmgGDS through β1-integrin/Akt1 pathway in endothelial cells. Cardiovasc Res. 2016 Jan 1;109(1):151–61.

160. Wang X-L, Qi J, Shi Y-Q, Lu Z-Y, Li R-L, Huang G-J, et al. Atorvastatin plus therapeutic ultrasound improve postnatal neovascularization in response to hindlimb ischemia via the PI3K-Akt pathway. Am J Transl Res. 2019;11(5):2877–86.